







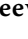



GEOINFORMATION ANALYSIS OF REGIONAL CLIMATIC CHANGES IN THE CENTRAL AND WESTERN RUSSIAN ARCTIC FOR RAILWAY DEVELOPMENT

A. G. Kostianoy^{1,2,3} , A. D. Gvishiani^{1,4} , I. N. Rozenberg⁵ , R. I. Krasnoperov¹ , S. A. Gvozdik^{*1,6} ,
S. A. Lebedev¹ , I. M. Nikitina¹ , I. A. Dubchak⁵, O. O. Shevaldysheva¹ ,
V. N. Sergeev¹ , and G. A. Gvozdik¹ 

¹Geophysical Center of the Russian Academy of Sciences, Moscow, Russia

²Shirshov Institute of Oceanology of the Russian Academy of Sciences, Moscow, Russia

³S. Yu. Witte Moscow University, Moscow, Russia

⁴Schmidt Institute of Physics of the Earth of the Russian Academy of Sciences, Moscow, Russia

⁵Russian University of Transport, Moscow, Russia

⁶Department of Earth and Environmental Sciences, University of Milano-Bicocca, Milan, Italy

* **Correspondence to:** Sofia Gvozdik, s.gvozdik@gcras.ru

Abstract: The Arctic Zone of the Russian Federation is characterized by the rapid growth of the mining industry, aimed at the extraction of oil, gas, coal, and ores, including rare earth metals. Railways are essential in the transportation of these resources to different regions of Russia for processing and export. Part of the cargo delivery is performed via the Arctic ports connected to the railway network. Rapid climate change, including regional climate warming, is among the compromising factors for the operation of the Arctic transport infrastructure. System analysis of climatic processes and assessment of potential hazards that they may induce requires adequate geoinformation support. This paper presents the results of spatio-temporal variability analysis of various hydrometeorological parameters for selected railway mainlines within the Arctic region. For this purpose, a new geoinformation method based on the Hovmöller diagrams was elaborated. This tool is useful for representing climate dynamics along the specified railway mainlines over several decades. It allows us to determine railway sections affected by anomalous climatic conditions on the variable time scale. The presented Hovmöller diagrams proved to be an efficient instrument for the regional climate change representation. It might be quite useful for railway infrastructure maintenance, planning, operation, and adaptation.

Keywords: Climate change, Russian Arctic, railway development, hydrometeorological parameters, GIS, Hovmöller diagrams, railway mainline analysis, transportation.

Citation: Kostianoy, A. G., A. D. Gvishiani, I. N. Rozenberg, R. I. Krasnoperov, S. A. Gvozdik, S. A. Lebedev, I. M. Nikitina, I. A. Dubchak, O. O. Shevaldysheva, V. N. Sergeev, and G. A. Gvozdik (2025), Geoinformation Analysis of Regional Climatic Changes in the Central and Western Russian Arctic for Railway Development, *Russian Journal of Earth Sciences*, 25, ES1005, EDN: OAMXSW, <https://doi.org/10.2205/2025es000956>

RESEARCH ARTICLE

Received: 26 November 2024

Accepted: 19 December 2024

Published: 28 February 2025



Copyright: © 2025. The Authors. This article is an open access article distributed under the terms and conditions of the Creative Commons Attribution (CC BY) license (<https://creativecommons.org/licenses/by/4.0/>).

1. Introduction

The Arctic zone of the Russian Federation (AZRF) is an interesting region in terms of its industrial and socio-economic development. Its area is about 4.2 million km². Here, indigenous peoples coexist, oriented toward preserving their traditional way of life, alongside rapidly developing modern projects interlinking industrial, tourism, and transportation growth. Severe weather conditions, climate change, and other features in the region impose constraints and demand heightened attention in conducting any activity [Yagova et al., 2023; Zonn et al., 2016, 2017]. The region's economic development is closely associated with the extraction of natural resources (oil, gas, coal, ores).

The Arctic contributes 15–20% to Russia's gross domestic product (GDP) [Kovalenko and Sibileva, 2023]. High transportation expenses considerably impede the advancement of remote northern regions, notwithstanding their abundant natural resources. The estimated share of freight traffic through the Northern Sea Route related to transporting these resources is 183.78 million tons by 2035, out of a total volume of 238.11 million tons. These aspects and “north delivery” practically account for 100% of the region's freight traffic through the Northern Sea Route [Decree..., 2022]. According to data in Transport of Russia [Ministry..., 2023], in 2022, railways accounted for 2639.4 billion ton-kilometers in total in Russia, which is 86.5% of the total cargo turnover by all modes of transport (excluding pipelines).

Many works note the impact of changes in climatic parameters on both planned railways and existing ones. For example, the effects of extreme temperatures on urban railway infrastructure assets are widely described in the work of Garmabaki [Garmabaki et al., 2024]. The study of climate change in railway areas is also considered using various models to create climate characteristics to determine the associated risks. For example, the approach of integrating meteorological parameters and operational factors to predict the degree of impact of various climate parameters on railway infrastructure [Kasraei et al., 2024].

As shown in [Gvishiani et al., 2023b,c], climatic changes in the Western and Central parts of the Russian Arctic are not uniform. Overall, warming in the Arctic region occurs at a rate of 2–3 times faster than the global average. Despite the Earth's general warming by approximately 0.8 °C, the Arctic has experienced a warming of up to 3 °C [Overland et al., 2014]. According to [Post et al., 2019], if the Earth's temperature rises by 2 °C, Arctic warming could reach an average of 4 °C, and during winter periods, it could reach up to 7 °C by 2100.

These changes have implications for the ecological, social, and economic systems of the region. Climate warming widens the scope for industrial activities and extends the available shipping periods by water transport. On the other hand, Arctic warming brings a range of negative consequences. It may lead to an increase in water levels and precipitation, intensification of stormy and wave activity, and permafrost degradation [Kattsov, 2022]. This will place greater stress on the existing infrastructure, including transportation networks [Kostianaia and Kostianov, 2023].

The paper considers selected lines of the main railway lines that have access to the promising ports of the Northern Sea Route, forming together a common logistics system (Figure 1). To select and correctly display the railway lines and major ports, the “Atlas of Railway lines” created by the Research and Design Institute of Informatization, Automation and Communications in Railway Transport (Moscow, Russia) and the Decree on Arctic Development Trends [Decree..., 2014; Rozenberg et al., 2019] were used (see Figure 1).

One significant inference drawn from the investigations conducted by [Gvishiani et al., 2023b,c] is that climate warming, along with alterations in other meteorological factors within the studied region, exhibits substantial irregularity on both temporal (monthly) and spatial scales, including variations along individual railway segments. It became clear that it is necessary to thoroughly study the climatic parameters along each railway section using so-called Hovmöller diagrams. The performed analysis has shown significant spatial and temporal heterogeneity of the considered parameters variability during the past 40 years.

The present study examines the changes in climate parameters (air temperature, atmospheric precipitation, wind speed, soil temperature, soil moisture content, air humidity, and snow thickness for 1980–2021) along the 7 major railway mainlines in the North-Western part of Russia (Table 1). This was done using the Hovmöller diagrams, which proved to be a very useful tool for such analysis.



Figure 1. Physical-geographical scheme of the study region. Dashed lines show the main railways. Yellow and red dashed lines show the location of the existing and planned railways studied in the present paper.

Table 1. Characteristics of the examined mainlines (see Figure 1 for location)

Examined lines	Total length of lines, km	Main railway	Cargo in 2023 by main railway, million tons
St. Petersburg–Murmansk	1385	Oktyabrskaya Railway	101.9 [Russian Railways, 2024b]
Yaroslavl–Arkhangelsk	833	Northern Railway	56.8 [Russian Railways, 2024a]
Kirov–Vorkuta–Salekhard	1621	Northern Railway	56.8 [Russian Railways, 2024a]
Saint Petersburg–Perm	1563	Sverdlovsk Railway / Gorky Railway	143.3 [Russian Railways, 2024c]
Tyumen–Novy Urengoy–Yamburg	1596	Sverdlovsk Railway	143.3 [Russian Railways, 2024c]
Yekaterinburg–Serov–Priobye	895	Sverdlovsk Railway	143.3 [Russian Railways, 2024c]
Salekhard–Novy Urengoy–Igarka–Dudinka (under construction)	1269	Northern Latitudinal Railway	–

2. Data and Methods

2.1. MERRA-2 Reanalysis

The research was based on the MERRA-2 reanalysis which was effectively used to analyze regional climate change in the AZRF [Gvishiani et al., 2023b,c]. The following monthly averaged meteorological parameters were considered: air temperature, atmospheric precipitation, wind speed, soil temperature, soil moisture content, air humidity, and snow thickness for 1980–2021.

The MERRA-2 reanalysis is the large catalog of climatic and meteorological data, which was recollected and reprocessed from the previous version – MERRA. Initiated by NASA's Global Modeling and Assimilation Office (GMAO), it aims to obtain and analyze historical meteorological and climatological data that was compiled over the last 40 years. The original MERRA project, starting in 1979, synthesized satellite measurements into a unified climate catalog. Discontinued in 2016 due to limitations, MERRA-2 emerged to ensure continuous near real-time climate monitoring, enhancing sensors and models [Gelaro et al., 2017; Ma et al., 2021]. MERRA-2 reanalysis data is an example of Big Data in Earth Science that is openly accessible to the global community, following the FAIR paradigm [Gvishiani et al., 2021, 2022, 2023a; Rybkina et al., 2018].

MERRA-2, an advanced atmospheric data collection, features upgraded equipment for measuring parameters and offers comprehensive temporal coverage since 1980. It emphasizes integrated methodologies to ensure data precision. The compilation process involves complex steps like data collection, assimilation, and validation [Ma et al., 2021].

Satellite observations, utilizing instruments like CrIS (Cross-Track Infrared Sounder) and ATMS (Advanced Technology Microwave Sounder), provide insights into air temperature and humidity at various altitudes [Han et al., 2013; Kim et al., 2014]. Modern precipitation measurement, incorporating radar satellite technology, enhances global atmospheric circulation models. MERRA-2 also utilizes surface data from GHCN (Global Historical Climatology Network) and CAMS (Climate Anomaly Monitoring System) [Bosilovich et al., 2016; Chen et al., 2002]. Specialized thermometers and remote sensing methods measure soil temperature, while soil moisture data are obtained through SMAP (Soil Moisture Active Passive Observatory) satellite observations [Dee and da Silva, 2003; Ma et al., 2021]. MERRA-2 employs normalized pseudo relative humidity for consistent atmospheric water content depiction. Snow cover thickness measurements consider snow characteristics and are presented with various adjustments [Bosilovich et al., 2016]. A more detailed description of specific observational and processing systems could be found in our previous works [Gvishiani et al., 2023b,c].

2.2. Hovmöller Diagrams

The Hovmöller diagrams are a convenient data representation for simultaneous analysis of spatial and temporal variability of various parameters for linear spatial objects. Such a chart was first described by Ernest Aabo Hovmöller (1912–2008), a Danish meteorologist, in 1949. He introduced a special type of meteorological diagram showing the longitude and intensity of cyclonic and anticyclonic systems in middle latitudes as a function of time [Hovmöller, 1949].

For decades the Hovmöller diagrams served for climatologists for the analysis of spatio-temporal variability of meteorological data [Hovmöller, 1949]. The original diagrams are plotted as follows. Time is usually recorded along the horizontal axis, while longitude, latitude, depth, height, pressure, etc. are plotted along the vertical axis. The alternate orientation of axes may also be used. The contour values of one of the physical or meteorological parameters may be presented through color or shading on this plot.

Definition 1. Extending the notion [Hovmöller, 1949] we can present a Hovmöller diagram as a function of two variables (1):

$$H_p = f(s, t), \quad (1)$$

where s is a parameter that takes values along a certain direction or line on a plane, t is time, and f is a 3D surface, represented by color or shading.

The domain of s is limited by the range of possible values of the plotted parameter (temperature, pressure, precipitation, etc.), and t is limited by the time interval for which the data for the parameter are available. The range of the function f is the space of qualitative or quantitative characteristics of the plotted parameter. The effective interpretation of the range of the function f is a color palette (e.g., from red – “dry” to blue – “wet” for precipitation, [Figure 2](#)) or a shading scheme for black and white schemes.

Such diagrams have been used for a long time to analyze climate change. [Jury et al. \[1991\]](#) have described wave-organized convective features in the Southwest Indian Ocean using Hovmöller composites of satellite imagery. [Chang and Orlanski \[1993\]](#) depicted the eddy vertical mean kinetic energy on Hovmöller diagrams and also showed the meridional component of the wind at 300 hPa. [Astafyeva and Rayev \[2009\]](#) have studied the Earth's radio-thermal field and the distribution of moisture and water storage in the troposphere based on similar spatial and temporal diagrams. For this purpose, the authors plotted the displacement of the most intense part of the intertropical convergence zone over the Atlantic for the period 1999–2005 along the 30°W meridian. The years were plotted along the horizontal axis and the latitude in degrees along the vertical axis. [Hocke and Kämpfer \[2009\]](#) have used atmospheric and oceanic reanalysis data for the past 60 years for the construction of the time latitude cross sections which inform about temporal and latitudinal variability, changes, and meridional circulation of the climate system on time scales from years to decades. [Shokurov and Germankova \[2015\]](#) used the diagrams of spatial and temporal variability to model the propagation of the gravity current in the compressible atmosphere. The diagram allowed them to describe the evolution of the potential temperature perturbation at 100 m in an experiment with an initial height of the cold region of 2 km. The propagation of the gravity current front was represented as a clear boundary separating air masses with different potential temperatures. In [\[Prants, 2021\]](#), Hovmöller diagrams were used to study the peculiarities of formation and behavior of synoptic anticyclonic eddies of deep-sea troughs. Hovmöller diagrams were also used by [Rankova et al. \[2022\]](#) to study the peculiarities of the temperature regime near the Earth's surface in 2021. In this work, the features of global warming were considered in the form of two-dimensional diagrams, where months were plotted on the horizontal axis and years on the vertical axis. Such a representation facilitated the study in detail of the changes in the surface temperature regime during the selected time interval.

The authors presume that the presented research is the first case of using the Hovmöller diagrams for the analysis of regional climate change along railways, which may have any orientation in space, any form, and any curvature. As a rule, parameters are analyzed either along parallels and meridians or for average values of a parameter over the whole selected study area. For railway construction, elevation profiles are often used, where the horizontal axis shows the kilometers of the selected railway line and the vertical axis shows the elevation. However, according to the results of the scientific literature search, the Hovmöller diagrams showing changes in climate parameters along the railway over time have not been previously constructed for railways. This paper uses the Hovmöller diagrams to study the spatial and temporal variability of hydrometeorological parameters along the selected main railways. The diagrams were compiled for the selected railway mainlines, see [Table 1](#). This provides a more detailed analysis of climate behavior regarding railway stations and an assessment of the influence of climatic parameters on the railway functioning at a particular point. This new methodology can be regarded as our know-how. Hovmöller diagrams in their modern interpretation can be used as an efficient tool in geoinformatics, which is successfully used to solve problems in geophysics, geodynamics, climatology, and other disciplines of the Earth sciences domain [\[Gvishiani et al., 2019\]](#).

The process of preparing the source data for the diagrams can be divided into several main stages: compiling a database for each climatic parameter for each railway line, combining the data into a single file, creating the final image, and subsequent processing. Golden Software Surfer was chosen as the main tool for creating Hovmöller diagrams [\[Golden Software LLC, 2024\]](#).

At the initial processing stage, shapefile (.shp) format GIS-compatible files containing coordinates of points along the railway line are generated. A smaller discretization step than the original MERRA-2 resolution was set to enhance field trend detail and consider track curvature. Sampling was performed at intervals of 5–10 km. Each shapefile was then used to sample monthly average hydrometeorological parameter values from a general dataset, resulting in files with discretization for each month. Data sampling was facilitated using a software module developed with Golden Software Surfer's Grid Slice function [Golden Software LLC, 2024]. The program automatically extracted values along the specified line from initial raster files, saving the results in .dat format. For each combination of climatic parameters and railway mainlines, were computed 504 files. Subsequent postprocessing was carried out using a specialized Python script. This script combined monthly files for selected railways and selected parameters into a unified database. These databases were subsequently converted through encoding modifications into files suitable for Hovmöller diagrams.

The third step involved constructing a single raster illustrating climatic parameter changes along the railway over time. Notably, the horizontal interval did not always align with the initial data grid, and the interval along the line was measured in kilometers. The minimum curvature gridding method was selected for constructing Hovmöller diagrams [Surfer Help, 2024]. This gridding method minimizes distortion in the interpolation area and represents data with maximum accuracy. The spatial resolution of the compiled diagrams is 15 km.

The obtained raster files were processed in the Surfer software package. For each climatic parameter, the color palette was set the same as in the schemes of climatic parameters (Table 2) used in [Gvishiani et al., 2023b,c]. This provides a comprehensive analysis of changes in hydrometeorological parameters for the entire study area, as well as separately for each railway mainline.

Table 2. Description of color palette

#	Parameter	Data limits	Color palette (min–max)
1	Air temperature	–26 to +25 °C	blue–white–red
2	Total precipitation	0 to 270 mm	red– yellow– blue
3	Wind speed	0 to 5 m/s	white–purple–blue
4	Soil temperature	–12 to +22 °C	blue–yellow–red
5	Soil moisture	18 to 44%	yellow–red–purple
6	Air humidity	0 to 14 g/kg	yellow–green–blue
7	Snow cover thickness	0 to 1.2 m	orange–green–purple

At this stage, the diagrams are ready for compilation into a single atlas and further analysis. Depending on the task, the diagram can be made more or less detailed on the vertical axis (t – time). Thus, if it is necessary to assess a parameter monthly variability along the railway track, the diagram is made for the specified year (Figure 2). In addition to analyzing changes in climatic parameters over time along the entire railway line, Hovmöller diagrams are convenient for estimating changes at different points on the railway at the same time. For example, from the beginning of July till August 2017 (Figure 2), low precipitation (10–20 mm) was recorded along almost the entire length of the railway, but the section of the railway from Igarka to Dudinka was more humid (30–40 mm of precipitation). Then, if it is necessary to analyze changes in the parameter over several years, there were diagrams for periods of not only one year but also 5 years. Displaying a longer period, e.g., 40 years, on the vertical axis provides an overall analysis of the change in the climatic parameters along the railway mainline over a long period. Such a graph is an apparent representation of climate warming or cooling, how chosen parameters change in a specified region over several decades, and whether there is a shift of seasons over time.

As a result, the entire Hovmöller diagram construction algorithm can be divided into several main stages:

1. Selecting a database considering the required catalog resolution (both in space and time). Defining the lines of interest along which the diagrams will be constructed.
2. Compiling a catalog, where a separate file is created for each time slice along the profile.
3. Combining files for each time slice into single files for each profile and each climatic parameter into .grd format files.
4. Formatting the resulting files into ready-made diagrams.

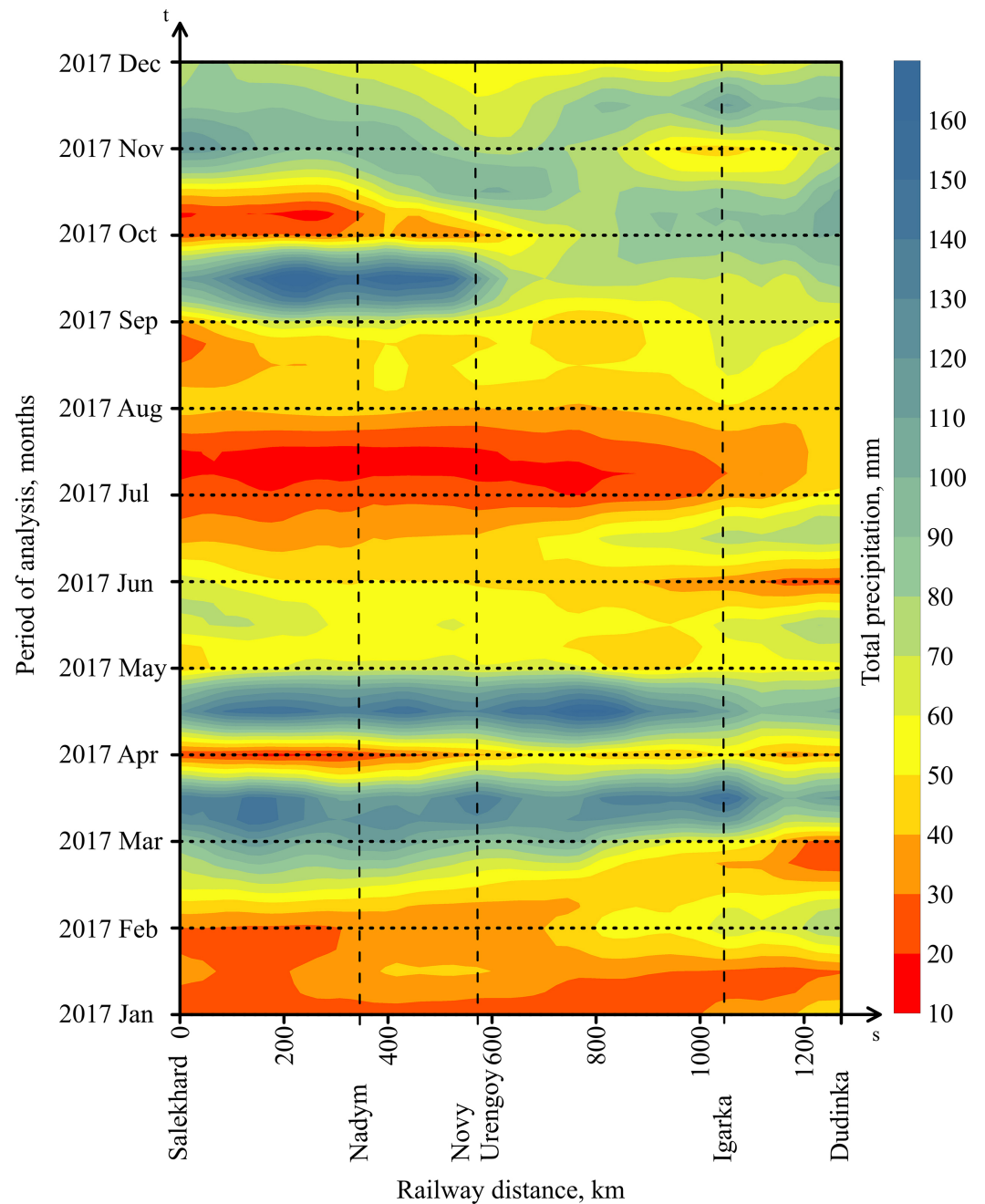


Figure 2. Hovmöller diagram of temporal variability of total atmospheric precipitation along the Salekhard–Novy Urengoy–Igarka–Dudinka railway mainline for the period January–December 2017.

3. Results

3.1. Hovmöller Diagrams for Railway Sections

In this article, we present the results of the analysis of Hovmöller diagrams of temporal variability of different hydrometeorological parameters along the seven-railway main lines, mentioned in the Introduction. In total, 49 diagrams have been constructed (7 railway lines by 7 meteo parameters), but in the paper, we demonstrate 7 of them which present the St. Petersburg–Murmansk mainline (Figs. 3–9) and additionally provide some interesting findings about other mainlines. To reduce the number of figures in the paper, the appropriate diagrams were presented in the [Appendix A](#).

3.1.1. Air Temperature

At the Saint-Petersburg–Murmansk railway mainline there is an evident increase in air temperature, which is not linear, but from year to year we observe that the Hovmöller diagram becomes redder ([Figure 3](#)). It means that at any point of the distance from Saint-Petersburg to Murmansk and in any season all months get to be warmer and warmer. For instance, the summer of 2010 which was the hottest during the previous decades, seems not to be very exceptional in comparison with the next summers in terms of the length of the warm period of the year and its temperature values. In general, air temperature decreases towards the north (Murmansk), and we did not find any exceptional (in terms of air temperature behavior) regions at this line.

So, for example, for the railway mainline Salekhard–Novy Urengoy–Igarka–Dudinka, which is under construction (see [Figure 1](#) for location), the Hovmöller diagram of air temperature from 2017 to 2021 ([Figure A1, Appendix A](#)) shows that: (1) the winter of 2020–2021 was significantly colder than in previous years; (2) the area to the east of Novy Urengoy is significantly colder in winter than the western section of the railway line; (3) the summer of 2019 was warmer than other years; (4) in the summer of 2020, the air temperature in the section between 700 and 1200 km of the track was higher than in the western section of the track; (5) in the summer of 2021, on the contrary, maximum temperatures were observed on the western section of the route, gradually decreasing from Salekhard to 900 km of the route.

3.1.2. Total Precipitation

The variability of the total precipitations in [Figure 4](#) shows the spatio-temporal variability of monthly mean total atmospheric precipitation along the Saint-Petersburg–Murmansk railway mainline. The diagram displays significant heterogeneity in time and along the distance from Saint-Petersburg to Murmansk. We do not observe evident drying or wetting of this region, but during years with significant positive or negative anomalies of precipitation, this occurs very irregularly along the railway and in time. Again, we did not find any exceptional (in terms of precipitation behavior) regions at this line.

Hovmöller diagram of temporal variability of total precipitation along the Kirov–Vorkuta–Salekhard railway mainline displays significant heterogeneity in time and along the distance from Kirov to Vorkuta ([Figure A2, Appendix A](#)). This is similar to the same diagram for the railway line between Saint-Petersburg and Murmansk ([Figure 4](#)). But we could detect a region between Pechora (1050 km) and about 1300 km where, in general, atmospheric precipitation is more intense. The second specific region is located between about 1500 km and Salekhard where total precipitation is an average low.

Analysis of the spatio-temporal variability of total precipitation Salekhard–Novy Urengoy–Igarka–Dudinka ([Figure A3, Appendix A](#)) showed that: (1) the spatio-temporal variability of precipitation on a given railway is very heterogeneous both in space and time; (2) minimal precipitation was observed in the winter of 2017/2018 and 2020/2021, and in the latter case from Salekhard to Novy Urengoy this period lasted from October 2020 to April 2021, and between Igarka and Dudinka – from December 2020 to April 2021; (3) the most wet periods (both in magnitude and duration) were observed in 2019, 2020 and 2021, with the highest precipitation values were in the western part of the road, and 2020 –

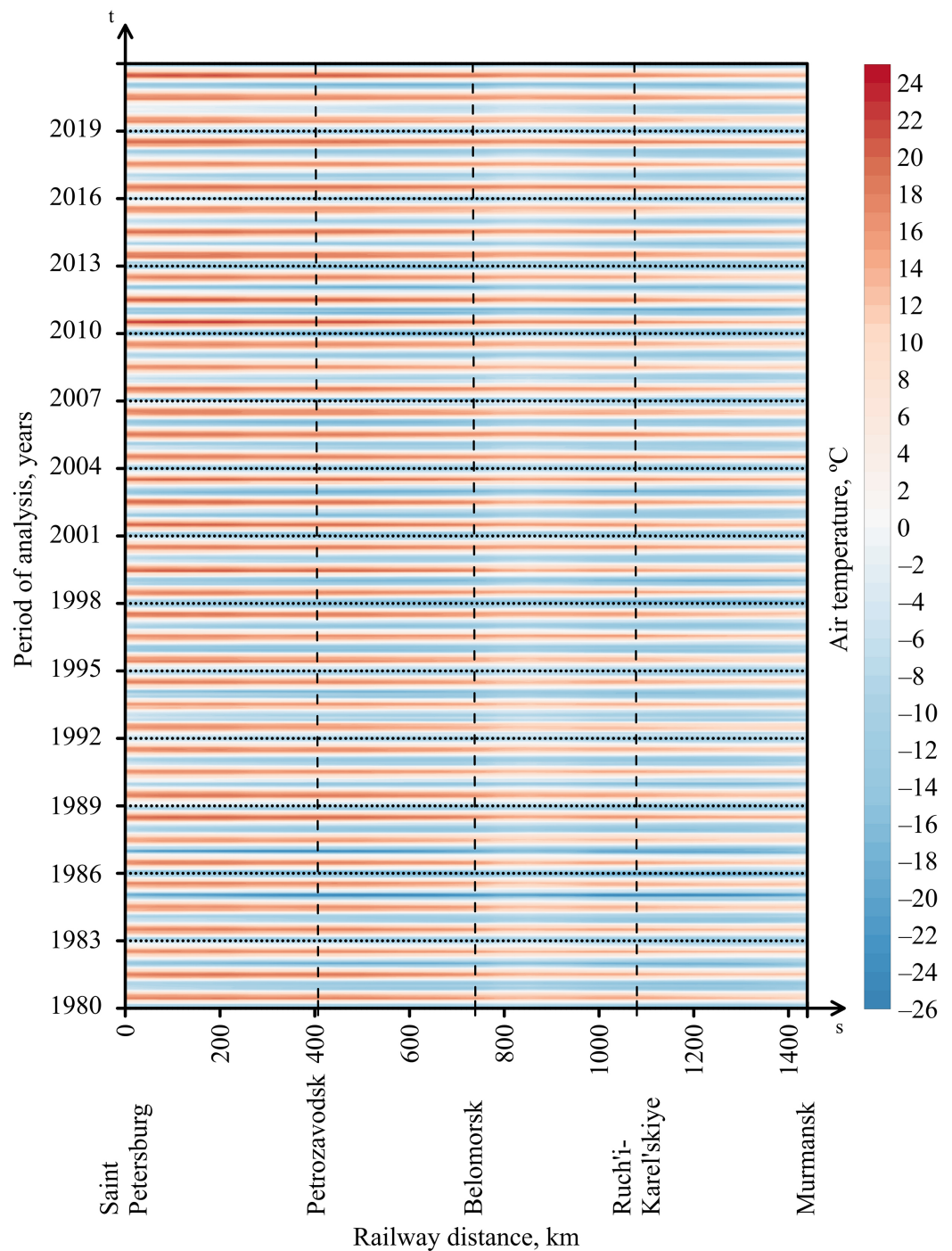


Figure 3. Hovmöller diagram of temporal variability of air temperature along the Saint-Petersburg–Murmansk railway mainline for the period 1980–2021.

in the eastern part; (4) in certain years, the wettest period may be briefly interrupted by a minimum of precipitation, for example, in July 2017 along the entire railway line, in July 2018 only in the section from Salekhard to Novy Urengoy, in July 2019, on the contrary, only from Novy Urengoy to Dudinka, in July 2020, only in the section from Salekhard to approximately 500 km of the track, and in 2021, the wet period was not interrupted at all.

3.1.3. Wind Speed

The spatio-temporal variability of monthly mean wind speed at Saint-Petersburg–Murmansk railway mainline is presented in Figure 5. There is an evident seasonal variability of wind speed with a maximum in wintertime. The diagram displays significant

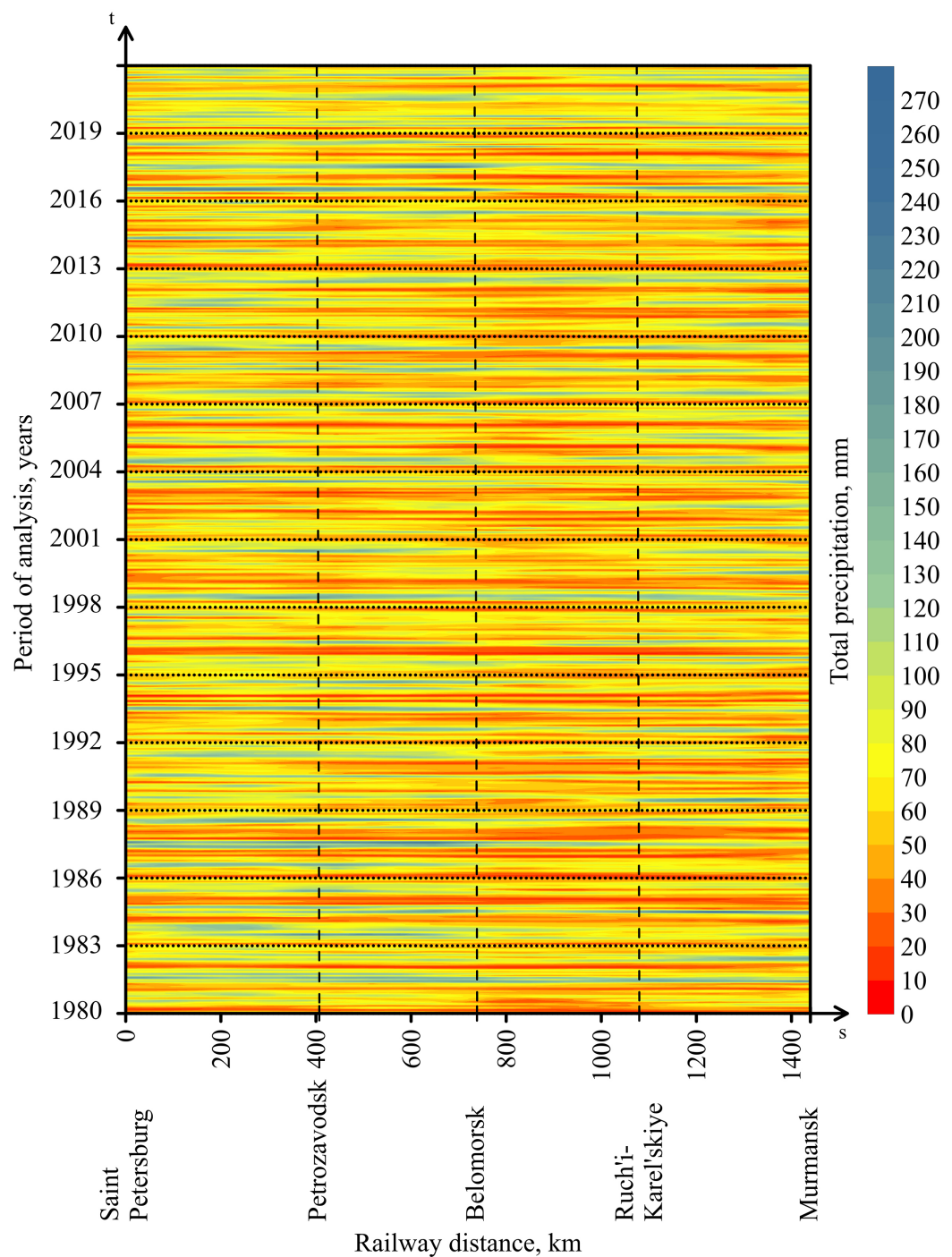


Figure 4. Hovmöller diagram of temporal variability of total atmospheric precipitation along the Saint-Petersburg–Murmansk railway mainline for the period 1980–2021.

heterogeneity along the railway line in the form of vertical bands with relatively higher or lower wind speeds in comparison with neighboring regions. For example, stronger winds are observed between 150 and 250 km, 750 and 950 km, and 1250 and 1450 km of the line. This phenomenon could be explained due to the proximity of the railway main line in these sections to large water bodies, such as Lake Ladoga, the White Sea, Lake Imandra, and Kola Bay.

Hovmöller diagram of temporal variability of wind speed along the Saint-Petersburg–Perm railway (Figure A4, Appendix A) has evident two vertical bands with, in general,

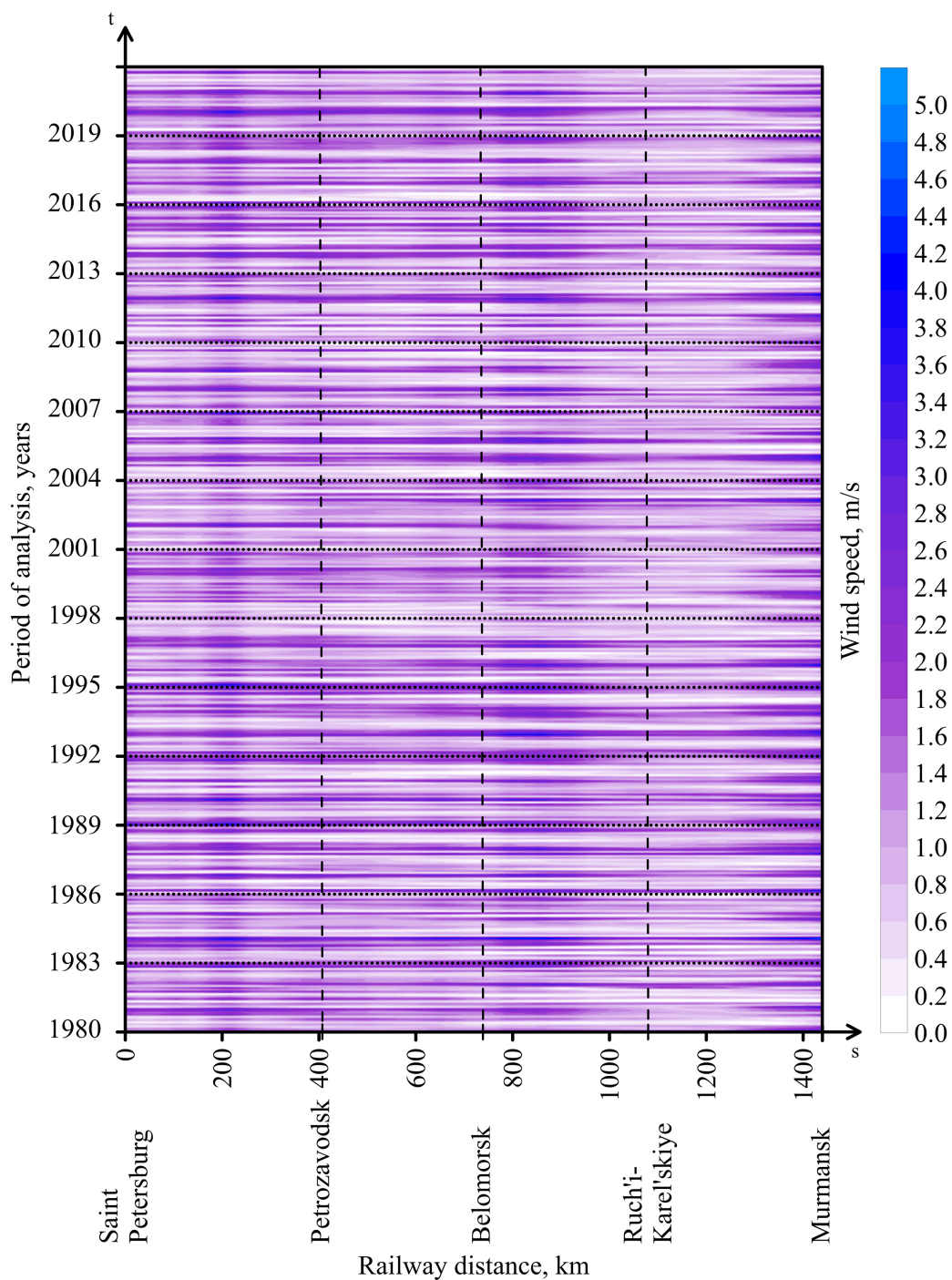


Figure 5. Hovmöller diagram of temporal variability of wind speed along the Saint-Petersburg–Murmansk railway mainline for the period 1980–2021.

higher wind speed values between 400–500 km and 1250–1400 km of the railway mainline. The high wind speeds between 400 and 500 km could be related to the fact that the railway runs along the shore of the Rybinsk Reservoir. Anomalous zone from 1250 to 1400 km could be described by a sharp change in elevation and the border zone with a forest belt. Seasonal variability of wind speed with the highest values in winter and lowest in summer is displayed in the diagram.

Spatial heterogeneity of wind speed along the Tyumen–Novy Urengoy–Yamburg railway mainline (Figure A5, Appendix A) is displayed by a strong difference in wind

regime over the first 250 km from Tyumen, as well as from about 1100 km to the end of the line in Yamburg, where wind speed is much higher than in the central part of the railway mainline. The high wind speed values from 1100 km onwards may be related to the railway approaching the ocean. We can pay attention to a separate band of higher wind speed between about 900–1000 km which confirms that a significant heterogeneity of wind speed does exist on the climatic periods on the scale of the order of 100 km.

3.1.4. Soil Temperature

Changes in soil temperature and its monthly variability at the Saint-Petersburg–Murmansk railway mainline are presented in [Figure 6](#). It is similar to the diagram for air temperature, and, in general, shows progressive warming of soil as well. There are no exceptional locations at this railway line similar to that found for wind speed.

Analysis of the spatio-temporal variability of soil temperature Salekhard–Novy Urengoy–Igarka–Dudinka ([Figure A6, Appendix A](#)) showed that: (1) soil temperature was maximum in the summer of 2019; (2) in the summer of 2018 and 2021 maximum soil temperatures were observed on the western section of the route, and in the summer of 2020, on the contrary, on the eastern section; (3) the winters of 2017 and 2021 were the coldest over these five years, and in the winter of 2018 a pronounced maximum of negative temperatures was observed only between Igarka and Dudinka.

3.1.5. Soil Moisture

[Figure 7](#) shows the spatiotemporal variability of monthly mean soil moisture at Saint-Petersburg–Murmansk railway line. We do not observe evident drying or wetting of this region with time, but we found evident heterogeneity along the railway line in the form of vertical bands with relatively higher or lower values of soil moisture. High soil moisture occurs between about 100 and 350 km of the line with a sharp boundary with the next track section. This is explained by the close location of Ladoga and Onega Lakes as the railway line passes between them. Other less pronounced two regions are located between about 550 and 750 km and around 900 km. Along these sections, the railway runs along the banks of bodies of water, such as the White Sea-Baltic Canal, or in areas with a large number of lakes.

Hovmöller diagram of temporal variability of soil moisture along the Yaroslavl–Arkhangelsk railway mainline ([Figure A7, Appendix A](#)) shows a significant large-scale heterogeneity along the line with many humid soils between about 300 and 550 km and 650–750 km. Year-to-year and seasonal variability modulates the limits of these two regions, this is why there are no strict boundaries for them. The increased soil moisture in these sections of the railway may be related to the large number of wetlands in this area. The diagram displays an interesting event between Yaroslavl (0 km) and about 250 km of the distance when in 2001–2004 there was a period with very dry soils which was not observed before or later, and it was not recorded during the same years at other parts of the railway line.

The spatiotemporal variability of soil moisture along the Ekaterinburg–Serov–Priobye railway mainline ([Figure A8, Appendix A](#)) does not observe evident drying or wetting of this region with time, but some years seem to be drier along the whole distance of the railway. For instance, this occurred in 1987, 1988, 2010, and 2013. We found evident heterogeneity along the railway line in the form of vertical irregular bands with relatively higher or lower values of soil moisture. In general, high soil moisture is observed at the first 200 km of the railway and from about 550 km to the end of the line in Priobye.

Analysis of the spatio-temporal variability of soil moisture content Salekhard–Novy Urengoy–Igarka–Dudinka ([Figure A9, Appendix A](#)) showed that: (1) the minimum soil moisture is located in the area between Nadym and approximately 850 km of the track (apparently, this is due to the physical and geographical features of the local landscape); (2) there is clear seasonal variability in soil moisture with a maximum from April to July each

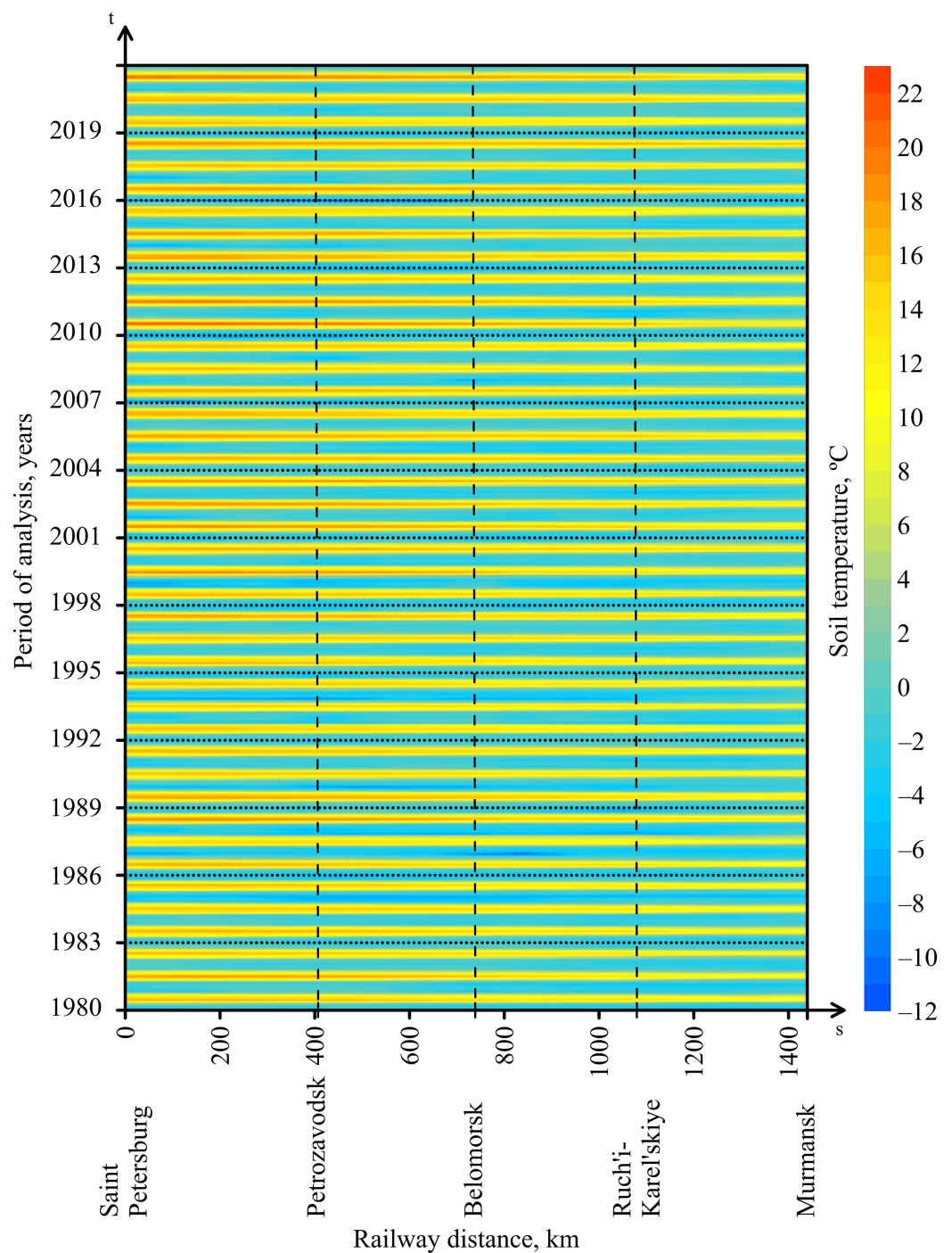


Figure 6. Hovmöller diagram of temporal variability of soil temperature along the Saint-Petersburg–Murmansk railway mainline for the period 1980–2021.

year; (3) in certain years, for example, in winter 2018/2019 and 2019/2020 increased soil moisture was also observed in the area of Salekhard and Dudinka.

3.1.6. Air Humidity

The variability of monthly mean absolute air humidity at the Saint-Petersburg–Murmansk railway line is presented in Figure 8. There is an evident seasonal variability of air humidity with a maximum in the warm period of the year and a minimum in the cold period of the year. The diagram does not display evident humidification or drying along

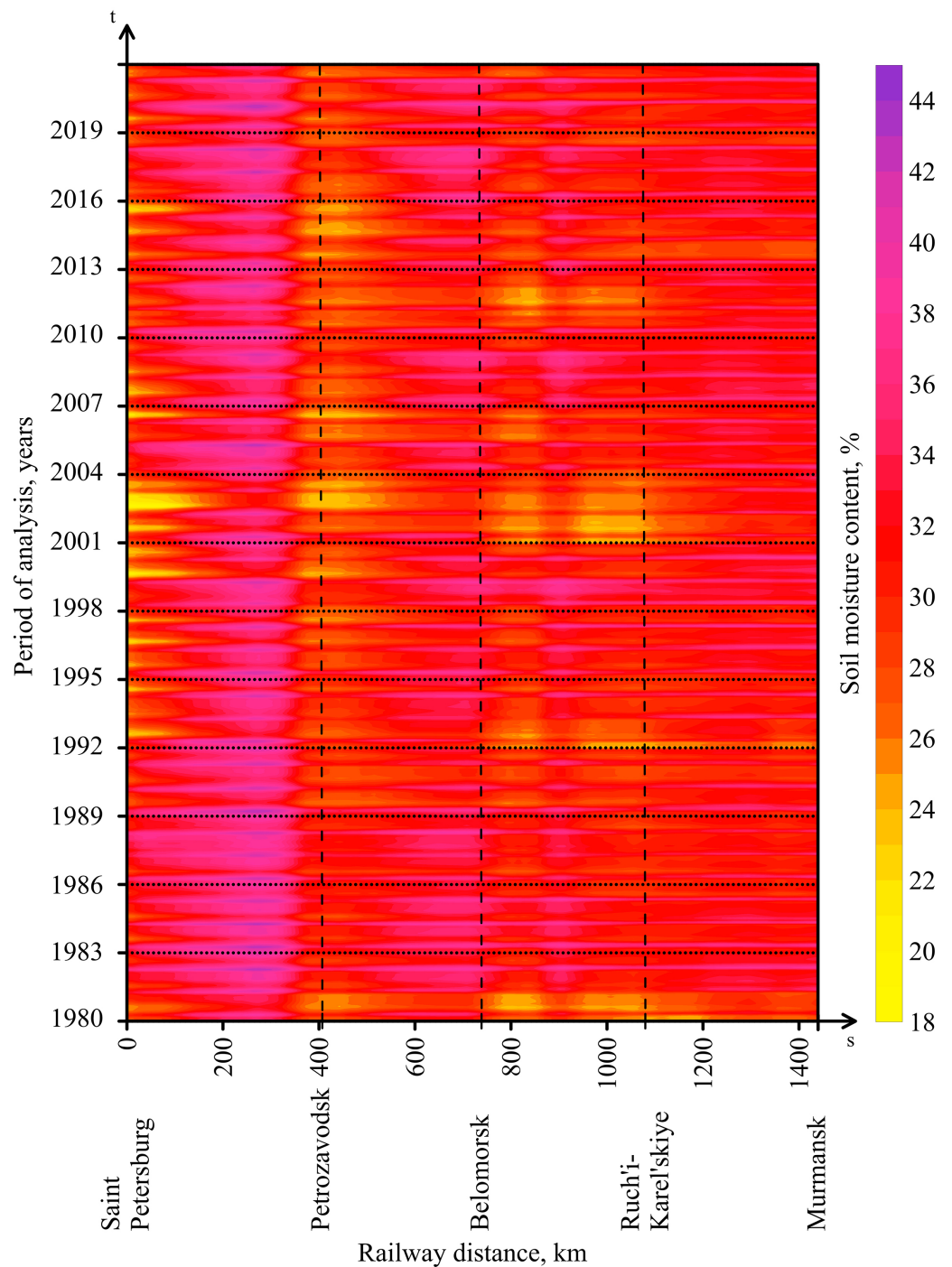


Figure 7. Hovmöller diagram of temporal variability of soil moisture along the Saint-Petersburg–Murmansk railway mainline for the period 1980–2021.

the railway line with time. In general, the southern part of the line is more humid than the northern one, which is explained by the proximity of the Baltic Sea, Ladoga, and Onega Lakes.

Analysis of the spatio-temporal variability of air humidity Salekhard–Novy Urengoy–Igarka–Dudinka (Figure A10, Appendix A) showed that: (1) there is a clear seasonal variability of air humidity with a maximum in the warm period of the year and a minimum in the cold period of the year; (2) there is no significant spatial variability of air humidity along the entire section of the track from Salekhard to Dudinka.

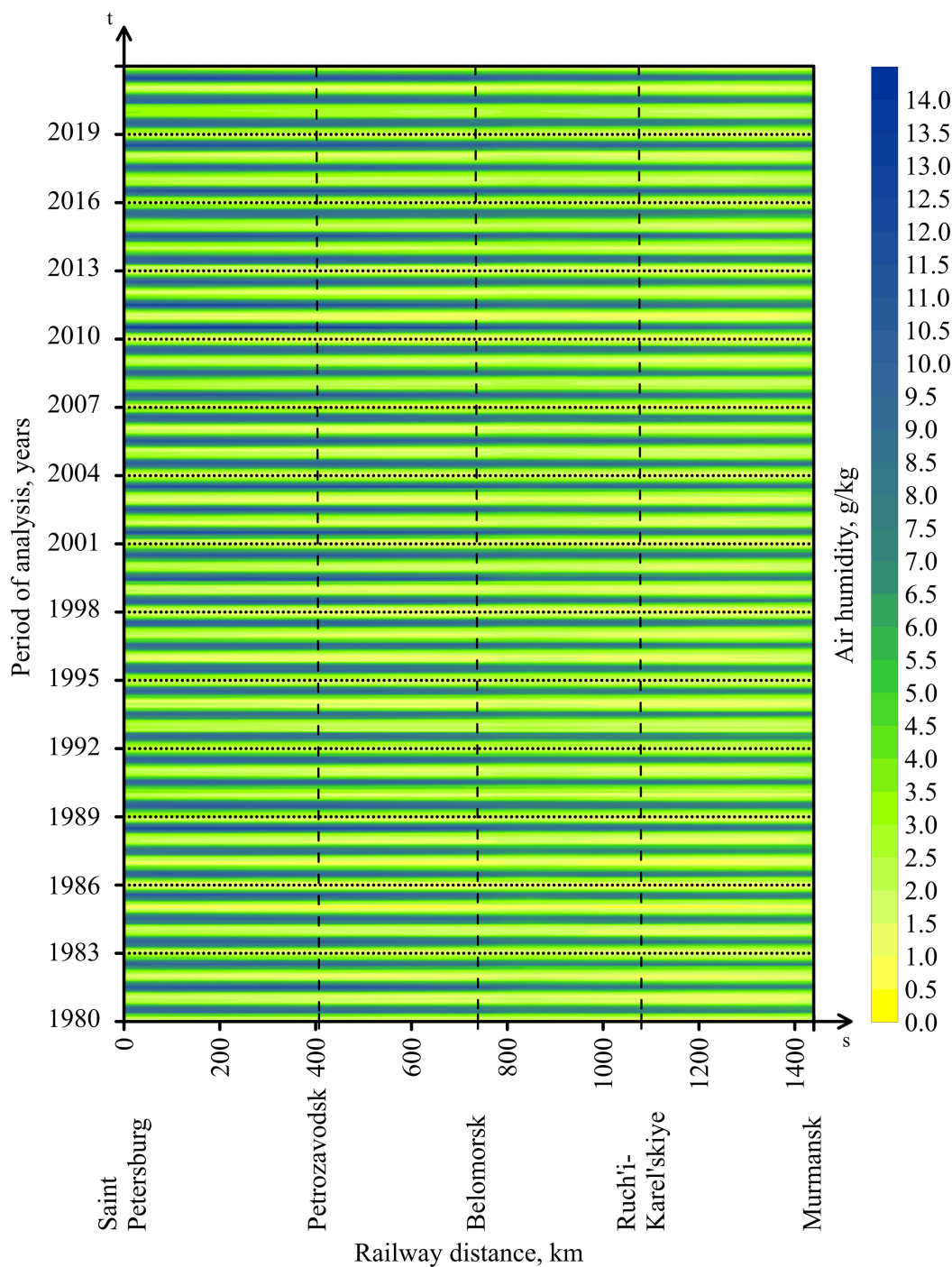


Figure 8. Hovmöller diagram of temporal variability of air humidity along the Saint-Petersburg–Murmansk railway mainline for the period 1980–2021.

3.1.7. Snow Cover Thickness

In **Figure 9** we present the spatio-temporal variability of monthly mean snow cover thickness (snow depth) at the Saint-Petersburg–Murmansk railway line. It is evident that snow is observed only in the wintertime, and with decades we have much longer snowless periods and snow depth goes down. It must be stressed, that a serious snow depth was observed in 1980–1984 in the southernmost part of the railway mainline (0–400 km), which we do not record in all subsequent years. On the other hand, significant year-to-year variability of snow depth remains in the northernmost part of the railway mainline (from

1100 km) with the largest snow depth anomaly in winter 2020, which was something exceptional since 1980. This fact confirms that with regional warming of the region anomalies in different meteo parameters may have significant values.

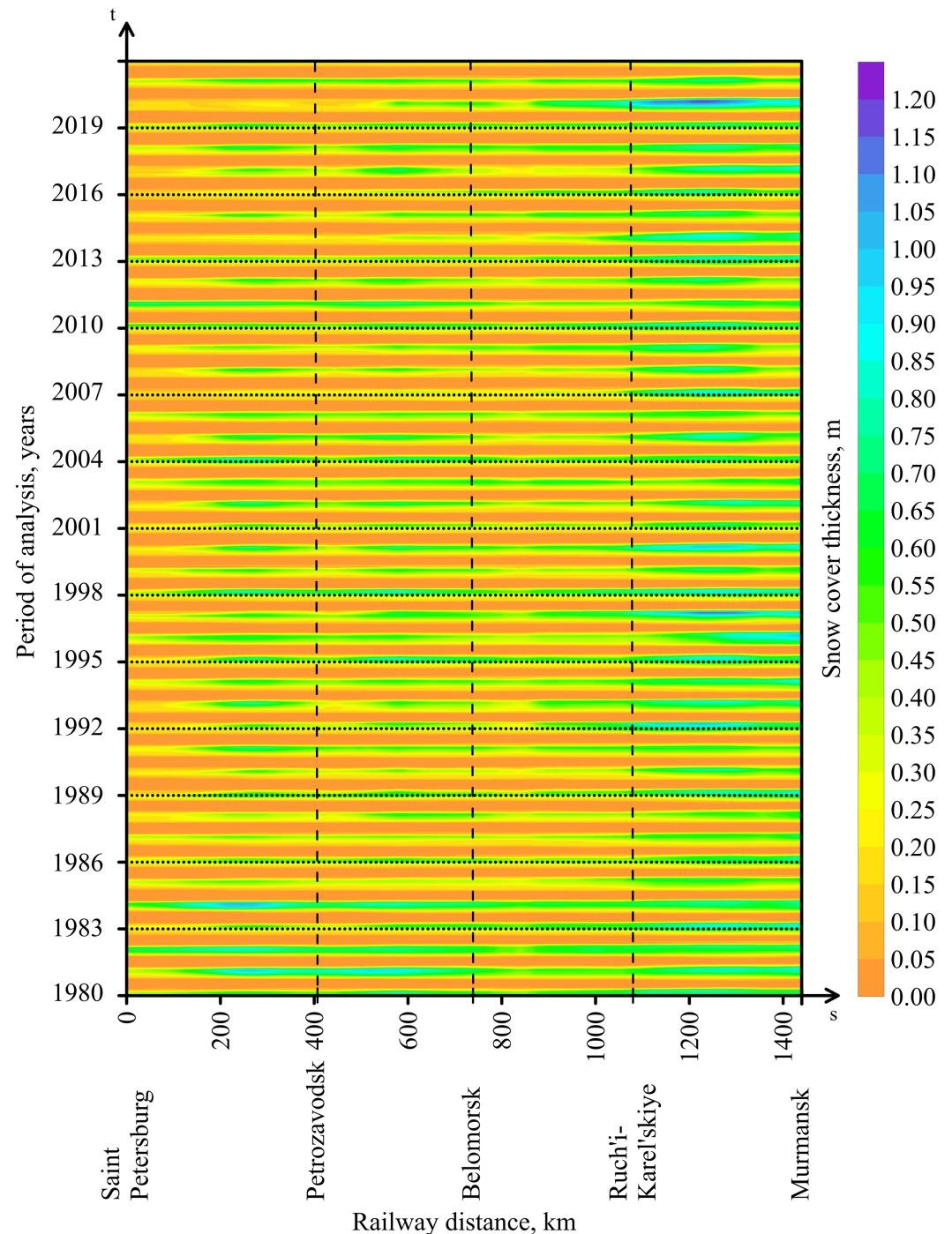


Figure 9. Hovmöller diagram of temporal variability of snow depth along the Saint-Petersburg–Murmansk railway mainline for the period 1980–2021.

Hovmöller diagram of temporal variability of snow depth along the Salekhard–Novy Urengoy–Igarka–Dudinka railway mainline (Figure A11, Appendix A) for the period 1980–2021) showed that: (1) there is an obvious seasonal variability of snow cover with a maximum in winter; (2) a significant maximum in snow cover is observed only in the area from approximately 900 km to Dudinka, and in the winter of 1985, 1999, 2010, 2013, and

2017 this maximum (blue colors) was not observed at all; (3) very snowy winters occurred in 1989, 1992, 1993, 1995, 1996, from 2002 to 2008, 2014, and from 2018 to 2020. Thus, snow depths of more than one meter can be found in the eastern part of the railway and this may occur very frequently. It seems that this factor will be the most important for the operability of railways in this planning part of the railway.

4. Discussion

The work of Gvishiani, Rozenberg, Soloviev, Kostianoy, et al. [Gvishiani et al., 2023b] has compiled an “Electronic atlas of climatic changes in hydro-meteorological parameters of the western part of the Russian Arctic for 1950–2021 as geoinformatics support of railway development”. Then, the improved version of this Atlas was used to study the impact of climatic changes in 1980–2021 on railway infrastructure in the Central and Western Russian Arctic [Gvishiani et al., 2023c]. In this paper, we went further and investigated the regional climate change that occurred during 1980–2021 in the Central and Western Russian Arctic namely along six existing railway mainlines and the one (NLR) that is under construction. All of them are in the northern part of the AZRF which is characterized by the rapid growth of the extractive industry. Railways play a key role in the transportation of these resources to different regions of Russia for processing and export. Part of the cargo delivery is performed via ports located on the Arctic coast of Russia, which are connected to the selected railway mainlines.

49 Hovmöller diagrams for 7 meteorological parameters listed in Table 2 for 7 railway mainlines were built. Being too bulky to provide and describe in this paper, they are presented as supplementary materials. The most distinctive findings after their analysis are the following.

Diagrams of atmospheric precipitation show large heterogeneity in time and space along the chosen railway mainlines.

The diagrams of wind speed and soil moisture display significant heterogeneity along the selected railway mainlines (Saint-Petersburg–Murmansk, Saint-Petersburg–Perm, and Ekaterinburg–Serov–Priobye) in the form of clear vertical bands of the order of 100–250 km with relatively higher or lower values in comparison with the neighboring regions. Sometimes these bands have relatively strict boundaries related to specific landscapes (lakes, mountains, valleys, etc.). In other cases, year-to-year and seasonal variability modulates the limits of these specific regions, which is why there are no strict boundaries for them.

The spatial stability of these bands during decades confirms that a significant heterogeneity of wind speed, soil moisture, and other meteo parameters exists on the climatic periods on the scale of 100 km.

The Hovmöller diagrams of temporal variability of different meteo parameters can be used for railway mainlines under construction or planning. It will allow us to assess the ongoing regional climate change along the future railway lines and to take measures for adaptation to future changes in the environment [Kostianaia and Kostianoy, 2023; Kostianaia et al., 2021].

We built Hovmöller diagrams for the railway mainline Salekhard–Novy Urengoy–Igarka–Dudinka (the NLR). Some sections of this mainline are under construction, and the other ones are under planning. In the Results, we described in detail the peculiarities of the ongoing changes in the regional climate between 2017–2021. Also, for the same railway mainline we built a graph of spatial variability of linear trends of changes of meteo parameters that occurred in 1980–2021 (Figure 10), which showed that the fastest changes occurred at the section Novy Urengoy–Igarka–Dudinka, which is under planning.

Figure 10 shows linear trends (per 10 years) of temporal variability of air temperature, total precipitation, wind speed, soil temperature, soil moisture, air humidity, and snow depth along the Salekhard–Novy Urengoy–Igarka–Dudinka railway mainline for the period 1980–2021. This representation of spatial variability of trends in temporal variability of

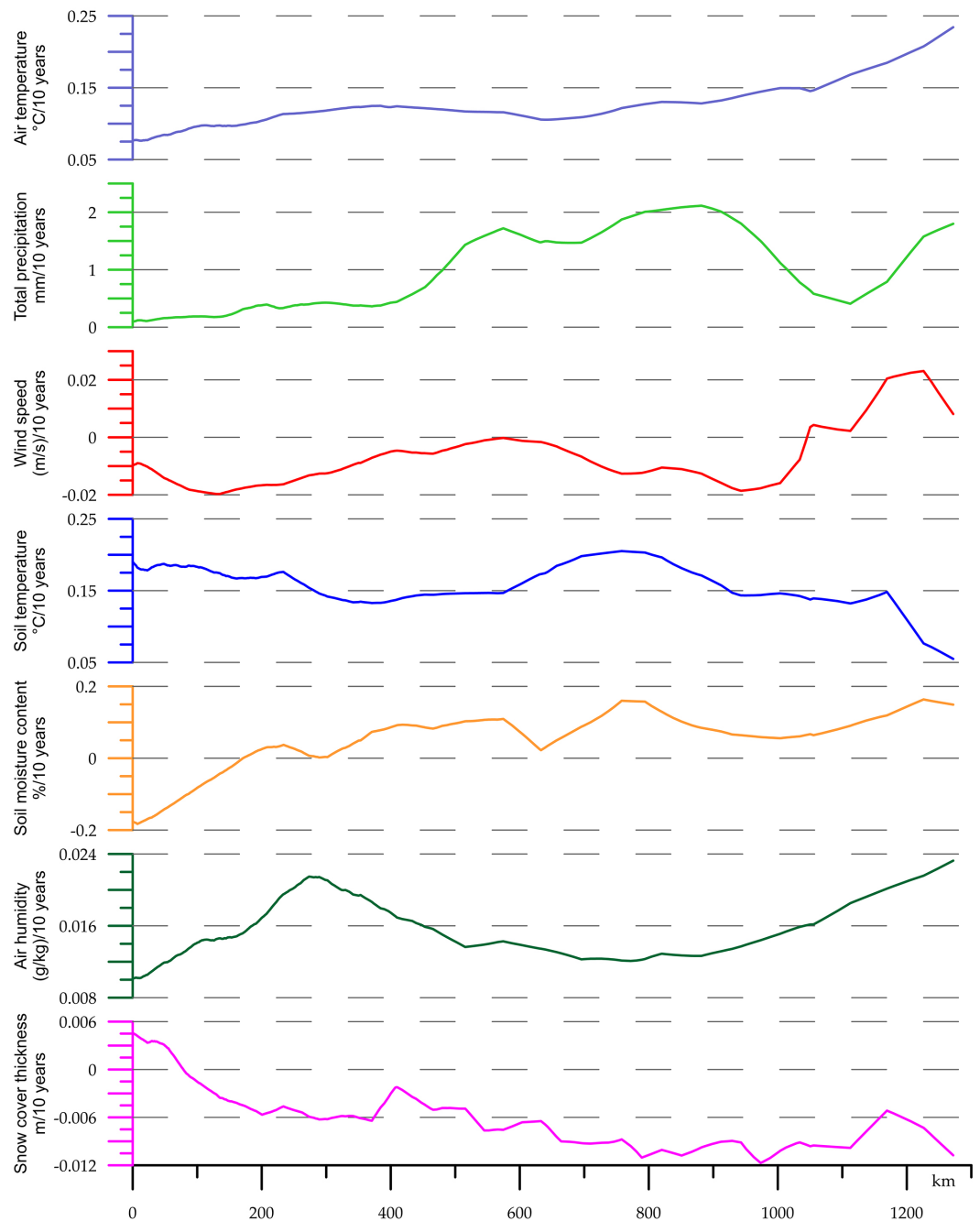


Figure 10. Linear trends (per 10 years) of temporal variability of air temperature, total precipitation, wind speed, soil temperature, soil moisture, air humidity, and snow depth along the Salekhard–Novy Urengoy–Igarka–Dudinka railway mainline for the period 1980–2021.

meteo parameters is also very important because it shows in what locations these changes are the strongest.

For instance, we can conclude that air temperature is rising everywhere and the largest growth of air temperature (over 0.25 °C/10 years) is observed eastward of Novy Urengoy. Atmospheric precipitation is increasing everywhere as well, except in a narrow region between approximately 600 and 700 km of the distance. Wind speed is decreasing with time everywhere except in the region between Igarka and Dudinka. Soil temperature is increasing along the whole line with a maximum in the interval between 600 and 950 km of distance and a minimum from 1150 km to Dudinka. Relative soil moisture is increasing everywhere (except for the first 100 km of the line) with two maxima at around 400 km and

750 km of the distance. Absolute air humidity is increasing as well with the highest rates in the eastern parts of the railway. With regional warming, snow depth is decreasing along the whole distance of the railway with the largest rates from Novy Urengoy to Dudinka. This type of plot is a more efficient way of representing regional climate change which might be very useful for railway infrastructure planning and adaptation.

5. Conclusions

The Hovmöller diagrams, introduced in 1949 [Hovmöller, 1949], are currently widely used by climatologists to study the variability of meteorological or climatic parameters along specific longitudes or latitudes. The authors presume that in this paper they were the first who proposed to use the Hovmöller diagrams for charting the temporal variability of meteorological parameters along selected railway mainlines which can go in any direction and have any number of bends in space. Thus, on the *X*-axis of the diagrams we plotted the railway track distance from the starting to the final station of the mainline. We used GIS software elaborated for this task to straighten the railway into a line (along the *X*-axis) and complete the Hovmöller diagram.

The compiled Hovmöller diagrams have a spatial resolution of 15 km of the railway line. The analysis of these diagrams for 1980–2021 for total atmospheric precipitation (on Kirov–Vorkuta–Salekhard and Saint-Petersburg–Murmansk railways), temporal variability of soil moisture (on Saint-Petersburg–Murmansk and Yaroslavl–Arkhangelsk railways), temporal variability of snow depth (on Saint-Petersburg–Murmansk and Salekhard–Novy Urengoy–Igarka–Dudinka railways), and others showed significant spatial heterogeneity of the order of 100–250 km in the form of bands (specific parts of the railway) persistent during decades.

A comparison of locations with anomalous meteorological parameters with geographic maps of the region showed that they relate to specific regions in the vicinity of seas, bays, lakes, etc., where the meteo regime of weather is different from the neighboring regions on a climate scale. One of the important conclusions based on this fact is that the spatial resolution of modern climate models often does not fully convey the variability of climate parameters depending on local geographic features. Since the spatial resolution of the models is on average 100–500 km, the detected bands of spatial heterogeneity of meteorological parameters may be lost due to the coarse mesh of the models.

The detected specific (anomalous) locations at the analyzed railway mainline must be taken under special control of railway operators with the establishment of additional weather and technical monitoring systems, especially in regions with higher precipitation and soil humidity, larger snow depth, and stronger wind speed. We believe that these locations will remain unchanged geographically in the future, but, unfortunately, future climate projections will probably not resolve them.

This new geoinformation climate methodology of the analysis of interannual variability of key meteo parameters, important for sustainable operability of railway infrastructure, can be applied to other regions of Russia and other countries where railway lines exist or are planned for construction. In the latter case detection of specific (anomalous) locations at certain segments of railway lines will allow in advance to take additional design decisions and safety measures during the construction of railway lines. It seems that such kind of Hovmöller diagrams must be constructed first for the historical period to detect these specific locations, and only then for future projections. The same geoinformation climate methodology can be applied to automobile roads which are subject to climate change as well.

Further research in this direction should be focused on the construction and analysis of Hovmöller diagrams showing anomalies of meteo parameters relative to the corresponding months. We expect that interesting results can be obtained from the Hovmöller diagrams constructed only for months that are key for certain parameters, for example, when air and soil temperatures pass through zero degrees Celsius or are below or over certain critical values. All this will make it possible to remove all seasonal variability from the Hovmöller

diagrams and leave only the interannual variability of the parameters under study, which will highlight the ongoing climate changes on certain sections of the railways. Finally, the application of such kind of Hovmöller diagrams for future climate change projections, for example, from the Coupled Model Intercomparison Project Phase 6 (CMIP6) is of vital importance for adaptation of the railway infrastructure to climate change in the Arctic conditions.

Acknowledgments. The research presented in this paper was funded by the Russian Science Foundation (Project No. 21-77-30010) “System analysis of geophysical process dynamics in the Russian Arctic and their impact on the development and operation of the railway infrastructure”. The authors wish to thank the faculty staff of the Russian University of Transport (Moscow) and the scientific team of the Research and Design Institute of Informatization, Automation and Communications in Railway Transport (Moscow, Russia) for providing valuable information on the railway infrastructure. The authors are grateful to the scientific teams of the responsible agencies and institutions for the provided climatic and hydrometeorological data.

Appendix A

This section contains additional figures (Hovmöller diagrams) that were not included in the main text of the paper (Figures [A1–A11](#)):

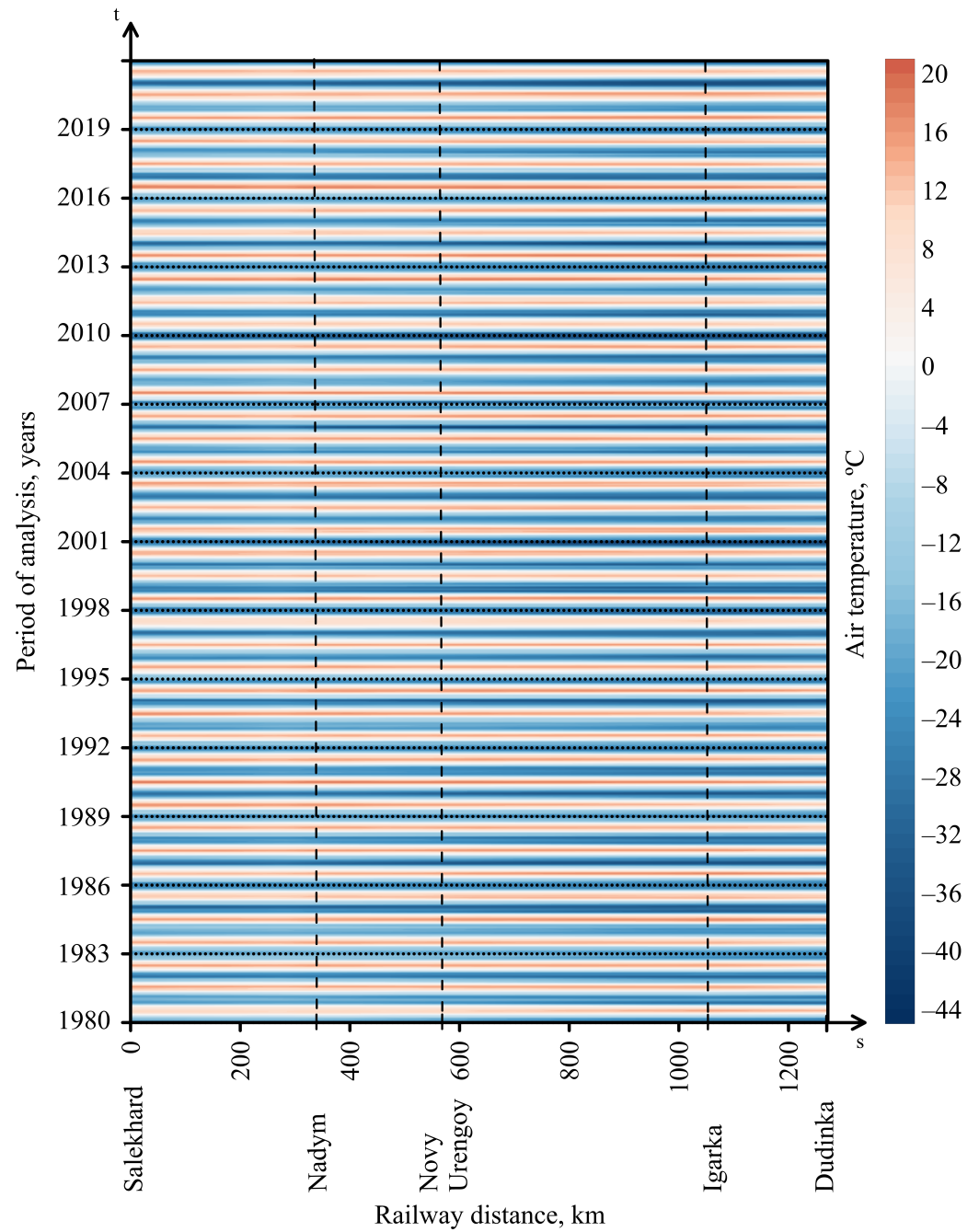


Figure A1. Hovmöller diagram of temporal variability of air temperature along the Salekhard–Novy Urengoy–Igarka–Dudinka railway mainline for the period 1980–2021.

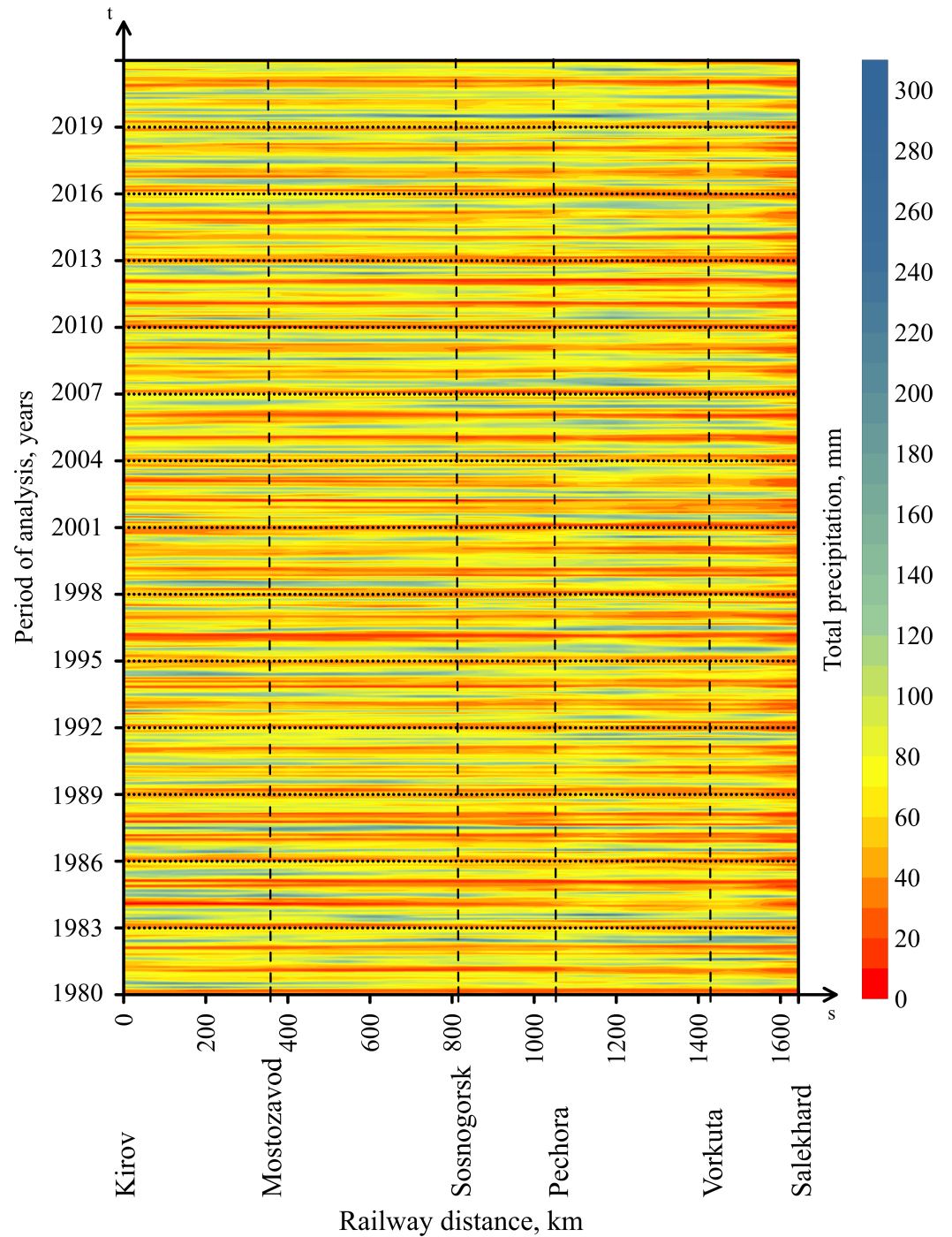


Figure A2. Hovmöller diagram of temporal variability of total atmospheric precipitation along the Kirov-Vorkuta-Salekhard railway mainline for the period 1980–2021.

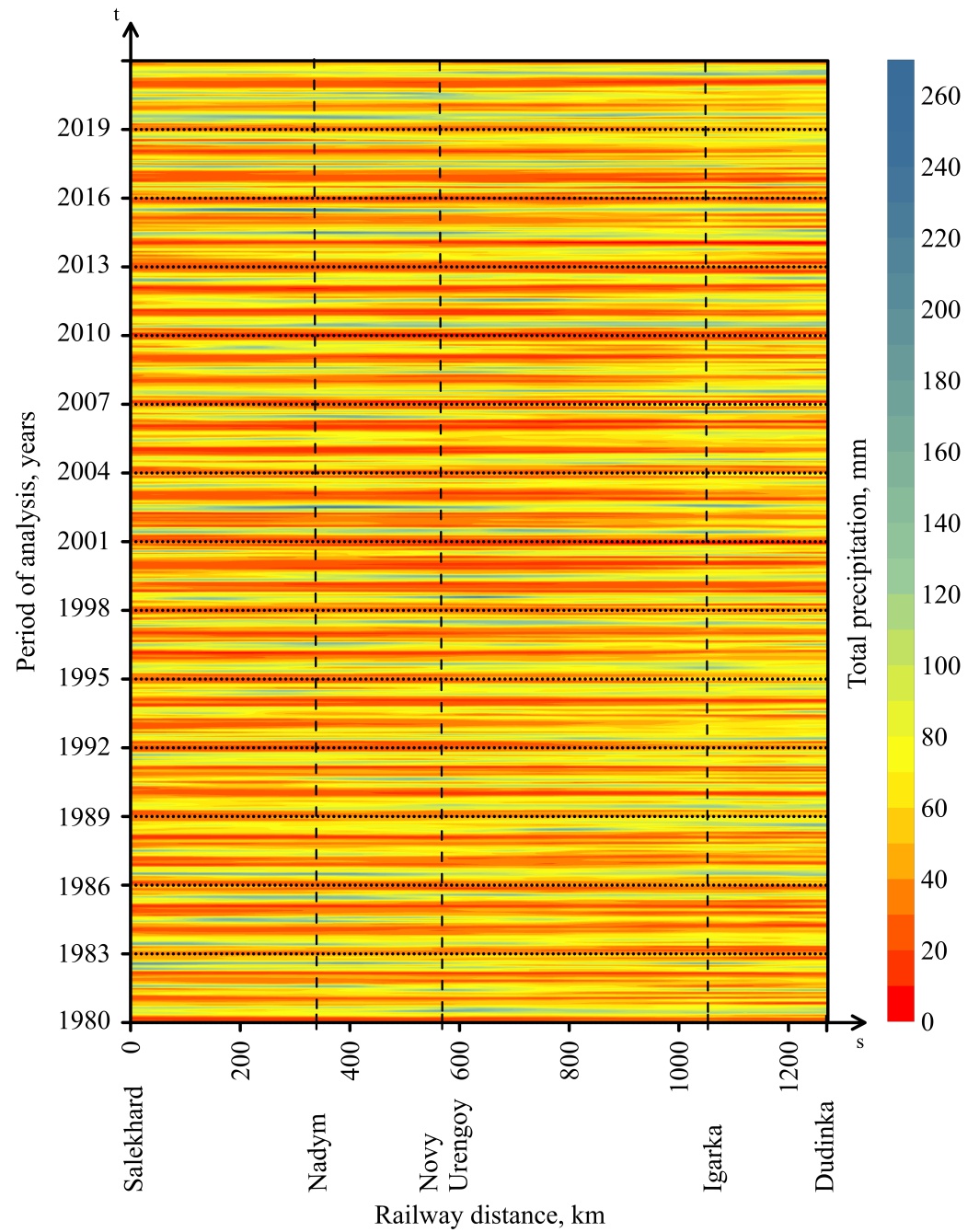


Figure A3. Hovmöller diagram of temporal variability of total atmospheric precipitation along the Salekhard–Novy Urengoy–Igarka–Dudinka railway mainline for the period 1980–2021.

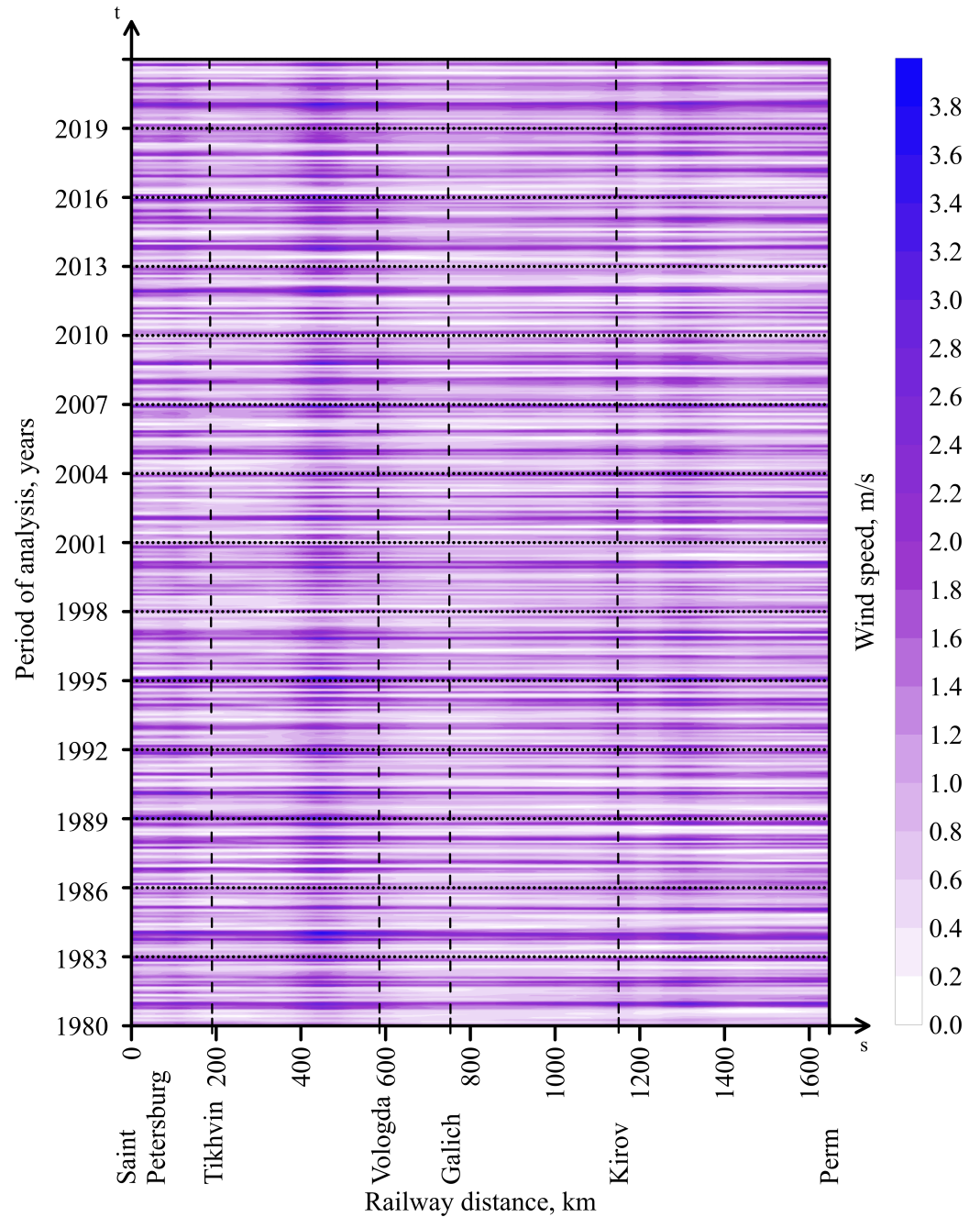


Figure A4. Hovmöller diagram of temporal variability of wind speed along the Saint-Petersburg–Perm railway mainline for the period 1980–2021.

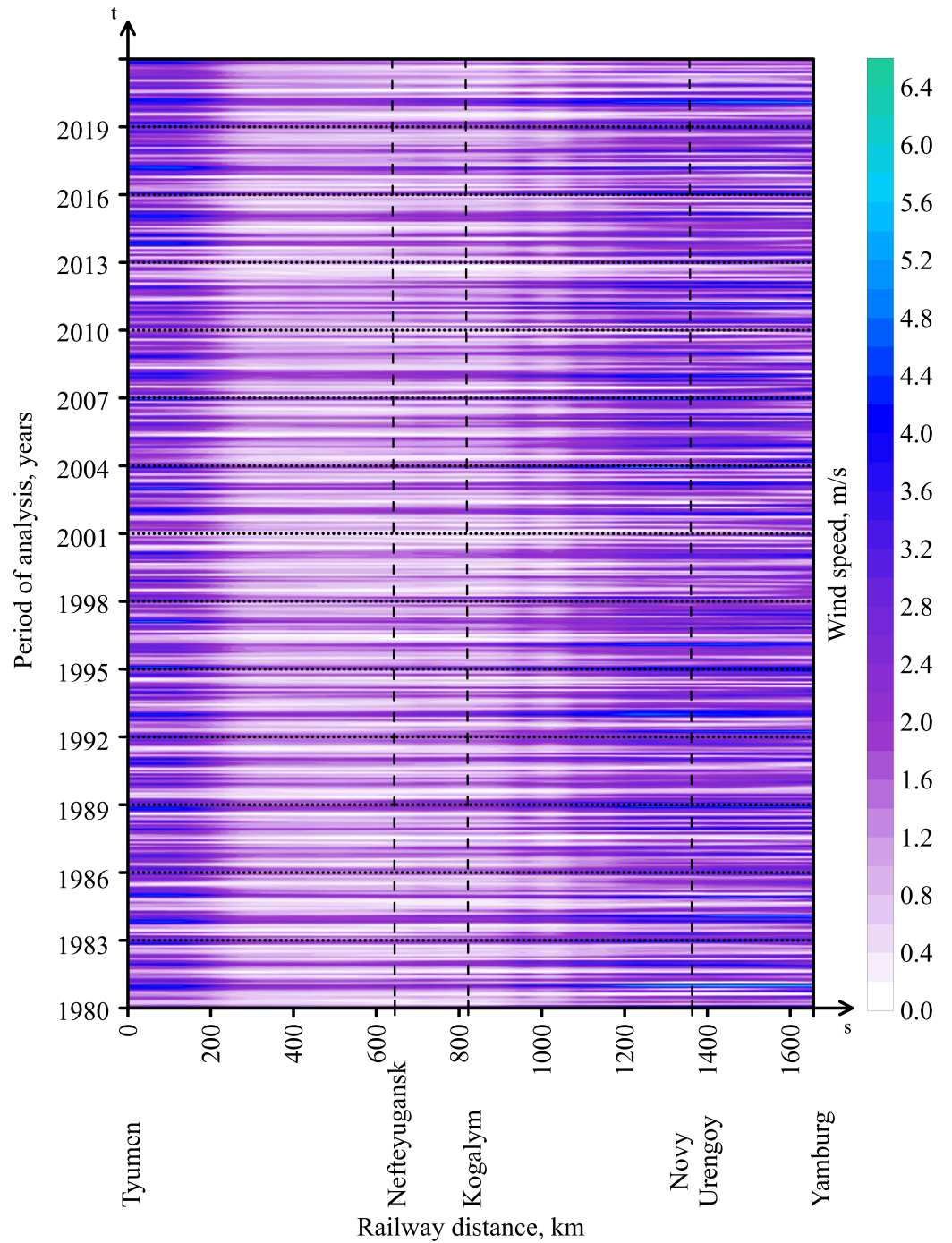


Figure A5. Hovmöller diagram of temporal variability of wind speed along the Tyumen–Novy Urengoy–Yamburg railway mainline for the period 1980–2021.

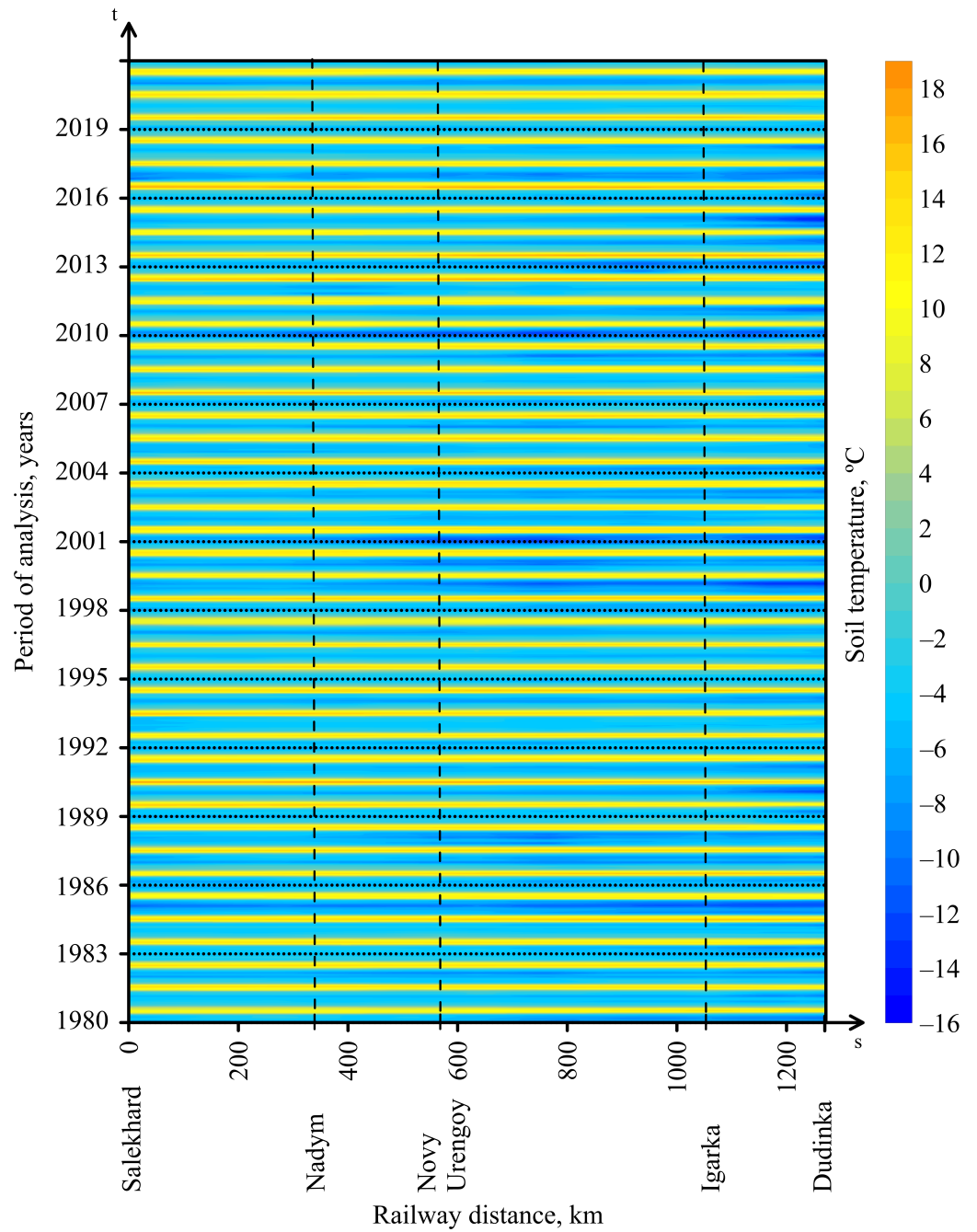


Figure A6. Hovmöller diagram of temporal variability of soil temperature along the Salekhard–Novy Urengoy–Igarka–Dudinka railway mainline for the period 1980–2021.

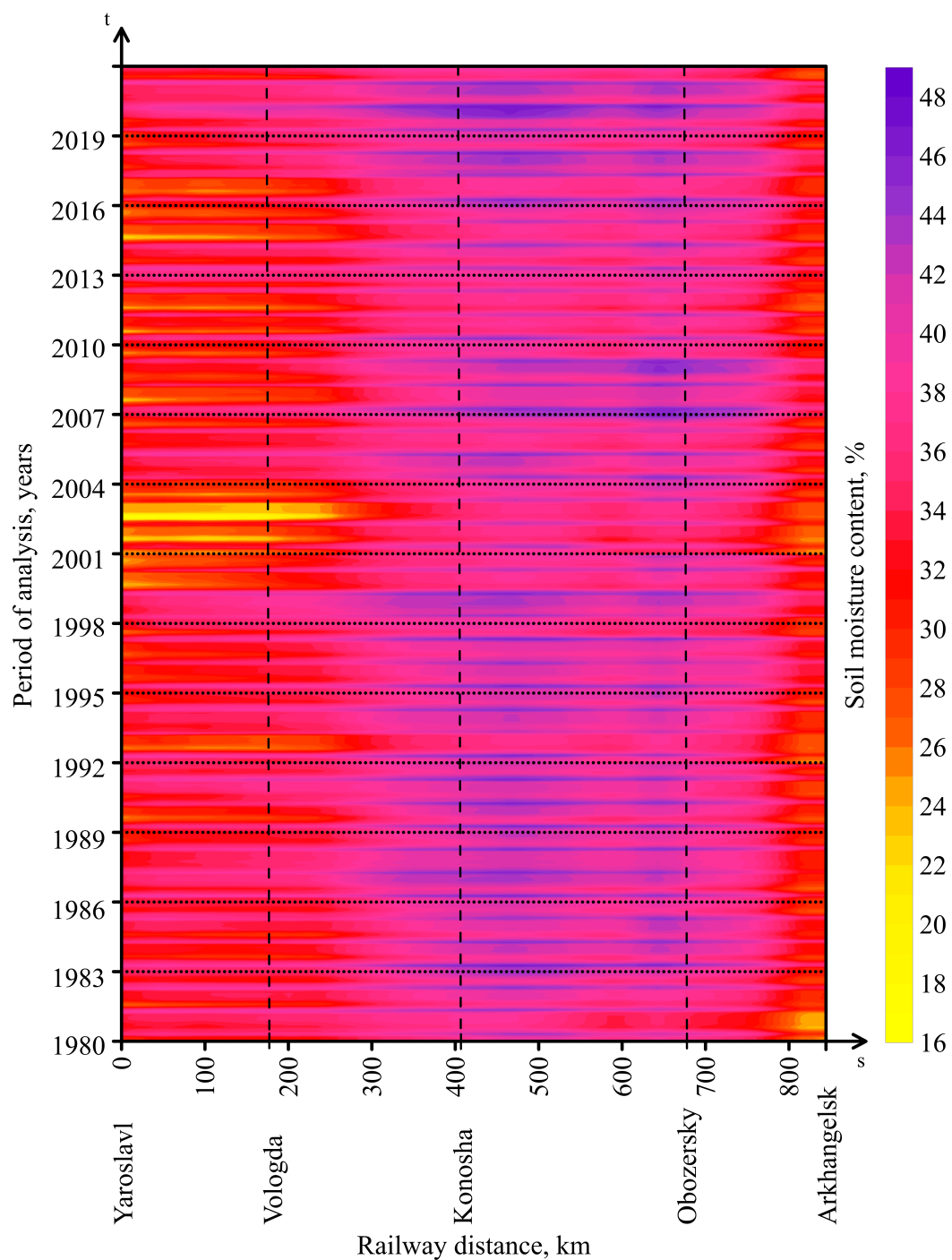


Figure A7. Hovmöller diagram of temporal variability of soil moisture along the Yaroslavl–Arkhangelsk railway mainline for the period 1980–2021.

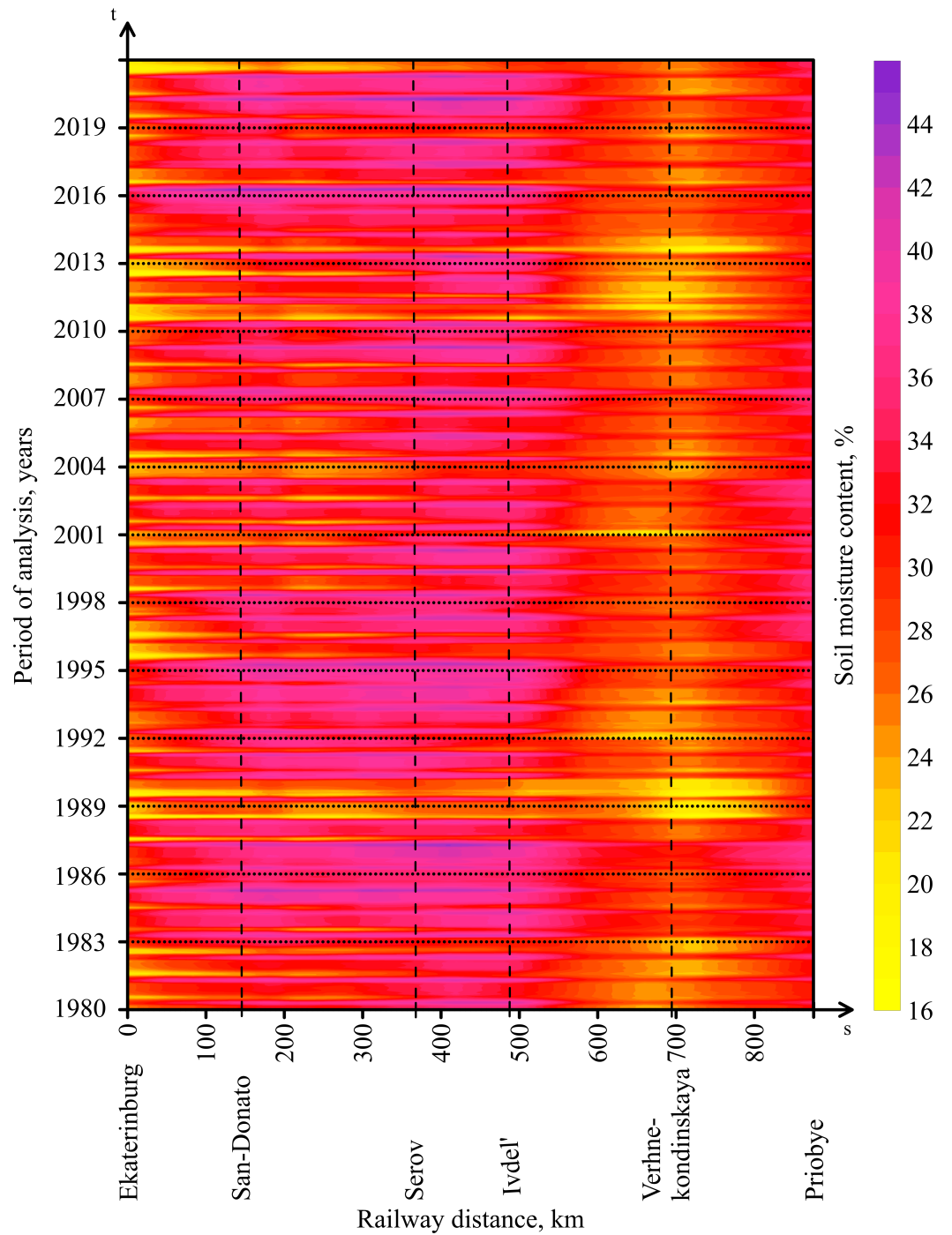


Figure A8. Hovmöller diagram of temporal variability of soil moisture along the Ekaterinburg–Serov–Priobye railway mainline for the period 1980–2021.

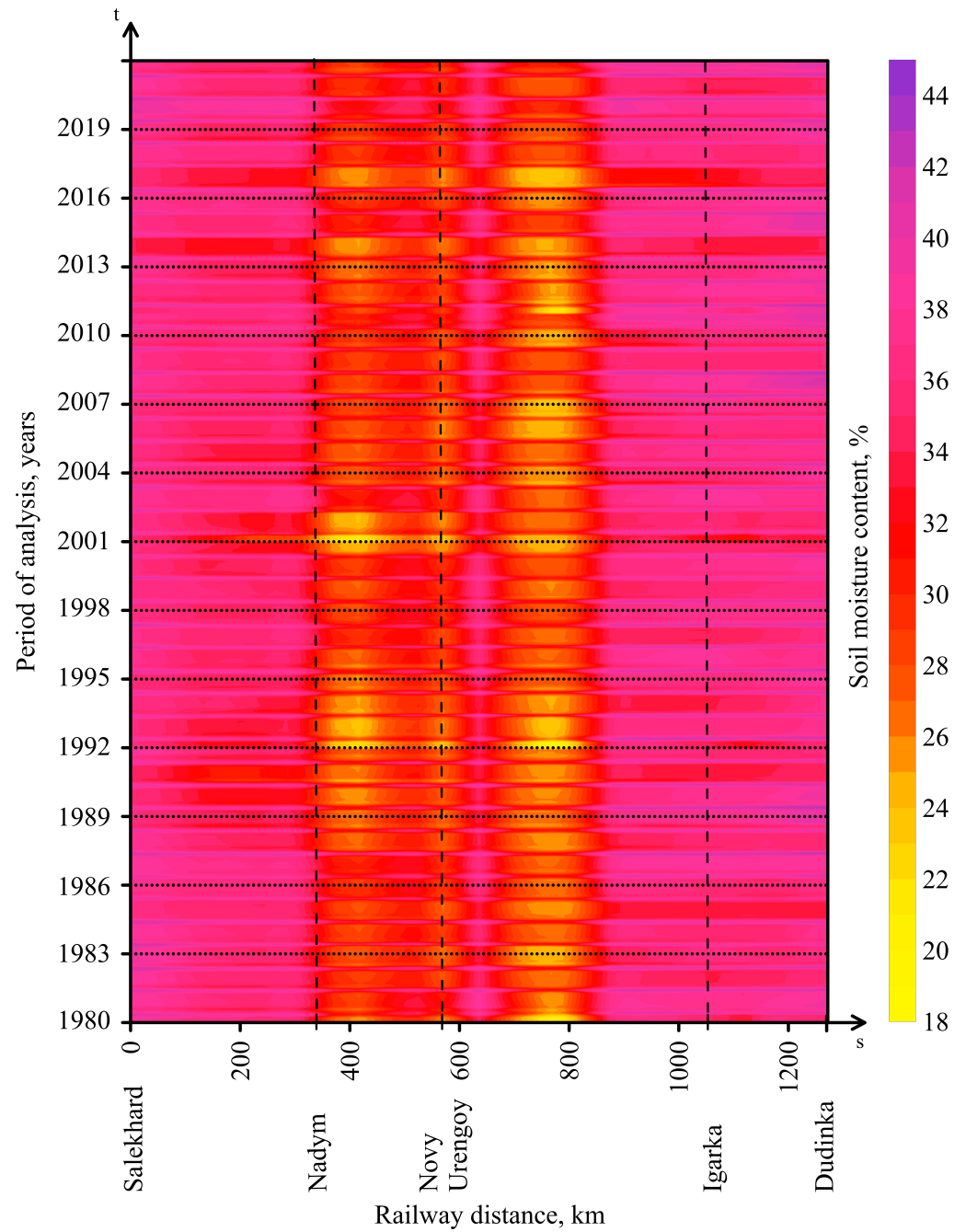


Figure A9. Hovmöller diagram of temporal variability of soil moisture along the Salekhard–Novy Urengoy–Igarka–Dudinka railway mainline for the period 1980–2021.

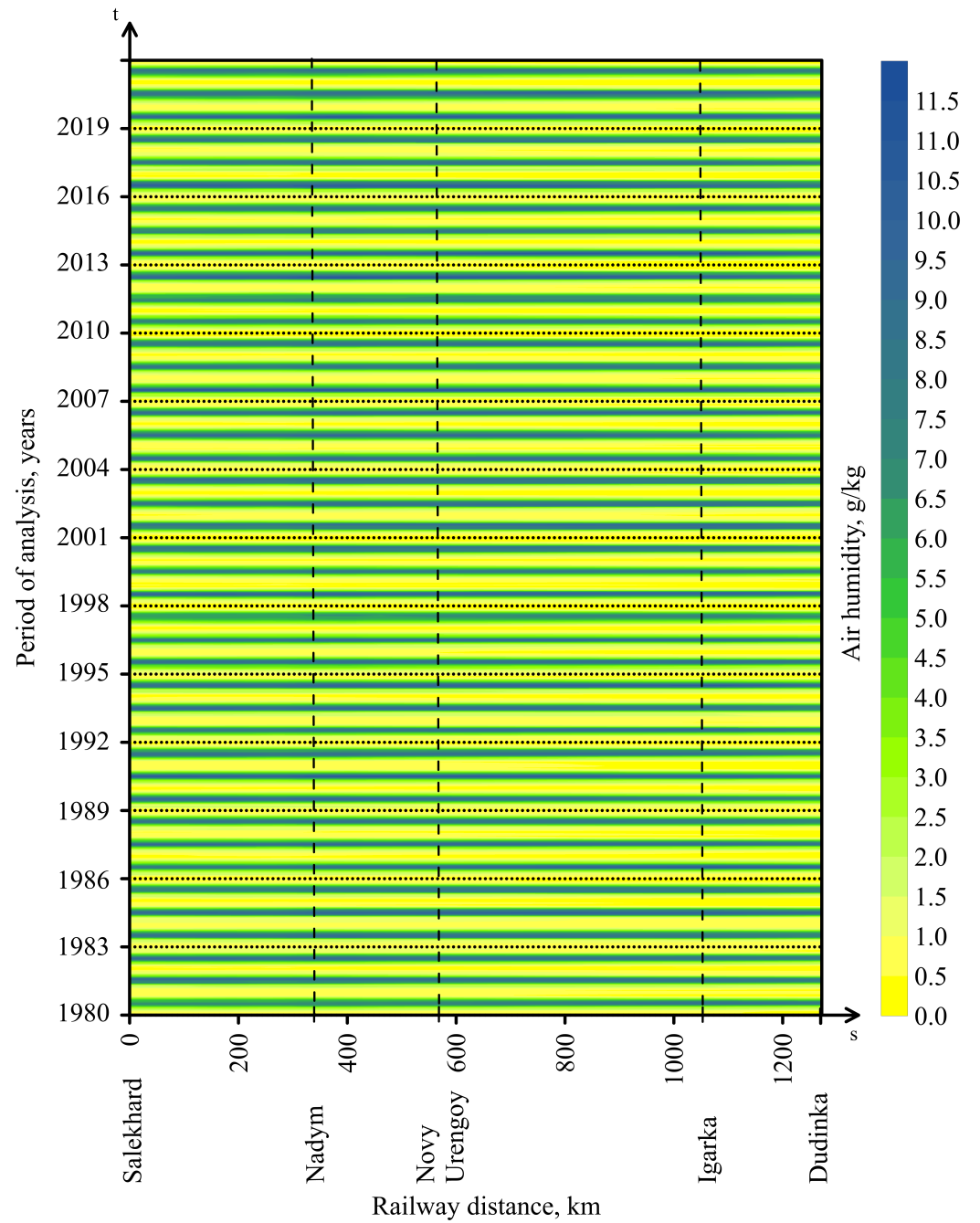


Figure A10. Hovmöller diagram of temporal variability of air humidity along the Salekhard–Novy Urengoy–Igarka–Dudinka railway mainline for the period 1980–2021.

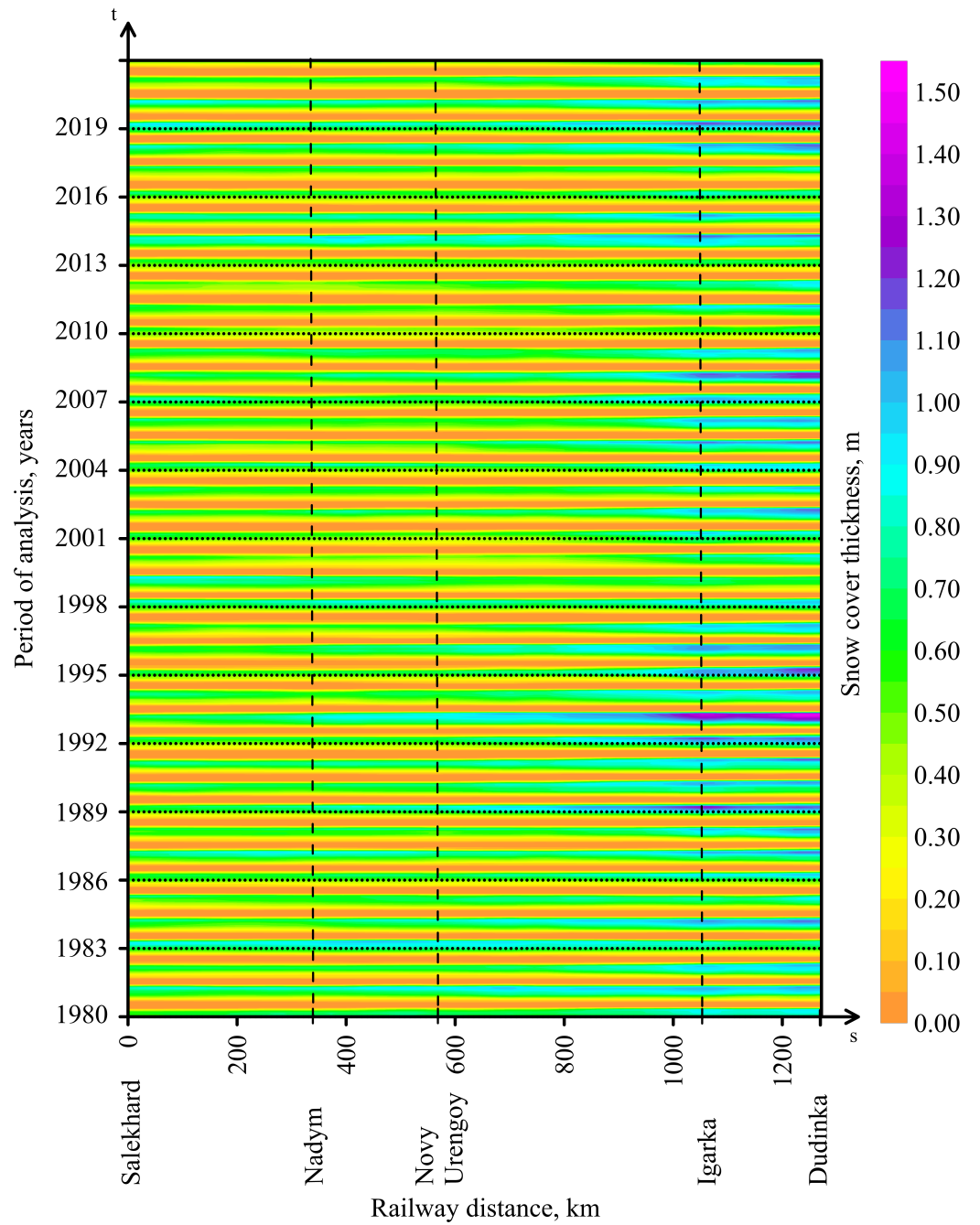


Figure A11. Hovmöller diagram of temporal variability of snow depth along the Salekhard–Novy Urengoy–Igarka–Dudinka railway mainline for the period 1980–2021.

References

- Astafyeva, N. M., and M. D. Rayev (2009), Methods of studying the Earth's radio-thermal field and distribution of tropospheric moisture storage, *Issledovanie Zemli iz kosmosa*, (6), 16–23 (in Russian).
- Bosilovich, M. G., R. Lucchesi, and M. Suarez (2016), *MERRA-2: File Specification*, GMAO Office Note No. 9 (Version 1.1).
- Chang, E. K. M., and I. Orlanski (1993), On the Dynamics of a Storm Track, *Journal of the Atmospheric Sciences*, 50(7), 999–1015, [https://doi.org/10.1175/1520-0469\(1993\)050<0999:OTDOAS>2.0.CO;2](https://doi.org/10.1175/1520-0469(1993)050<0999:OTDOAS>2.0.CO;2).
- Chen, M., P. Xie, J. E. Janowiak, and P. A. Arkin (2002), Global Land Precipitation: A 50-yr Monthly Analysis Based on Gauge Observations, *Journal of Hydrometeorology*, 3(3), 249–266, [https://doi.org/10.1175/1525-7541\(2002\)003<0249:GLPAYM>2.0.CO;2](https://doi.org/10.1175/1525-7541(2002)003<0249:GLPAYM>2.0.CO;2).
- Decree of the Government of the Russian Federation of 01.08.2022 No. 2115-r (as amended on 28.04.2023) (2022), On approval of the Development Plan of the Northern Sea Route for the period up to 2035 (in Russian).
- Decree of the President of the Russian Federation dated 02.05.2014 No. 296 (2014), On the land territories of the Arctic zone of the Russian Federation (in Russian).
- Dee, D. P., and A. M. da Silva (2003), The Choice of Variable for Atmospheric Moisture Analysis, *Monthly Weather Review*, 131(1), 155–171, [https://doi.org/10.1175/1520-0493\(2003\)131<0155:TCOVFA>2.0.CO;2](https://doi.org/10.1175/1520-0493(2003)131<0155:TCOVFA>2.0.CO;2).
- Garmabaki, A. H. S., M. Naseri, J. Odellius, et al. (2024), Assessing climate-induced risks to urban railway infrastructure, *International Journal of System Assurance Engineering and Management*, <https://doi.org/10.1007/s13198-024-02413-9>.
- Gelaro, R., W. McCarty, M. J. Suárez, et al. (2017), The Modern-Era Retrospective Analysis for Research and Applications, Version 2 (MERRA-2), *Journal of Climate*, 30(14), 5419–5454, <https://doi.org/10.1175/JCLI-D-16-0758.1>.
- Golden Software LLC (2024), Surfer. Create an immersive 2D/3D model in under 2 minutes, <https://www.goldensoftware.com/products/surfer>.
- Gvishiani, A. D., V. I. Kaftan, R. I. Krasnoperov, V. N. Tatarinov, and E. V. Vavilin (2019), Geoinformatics and Systems Analysis in Geophysics and Geodynamics, *Izvestiya, Physics of the Solid Earth*, 55(1), 33–49, <https://doi.org/10.1134/S1069351319010038>.
- Gvishiani, A. D., M. Dobrovolsky, and A. Rybkina (2021), Chapter 6 Big Data and FAIR Data for Data Science, in *Resilience in the Digital Age*, pp. 105–117, Springer International Publishing, https://doi.org/10.1007/978-3-030-70370-7_6.
- Gvishiani, A. D., M. N. Dobrovolsky, B. V. Dzeranov, and B. A. Dzeboev (2022), Big Data in Geophysics and Other Earth Sciences, *Izvestiya, Physics of the Solid Earth*, 58(1), 1–29, <https://doi.org/10.1134/S1069351322010037>.
- Gvishiani, A. D., V. Y. Panchenko, and I. M. Nikitina (2023a), System analysis of big data for Earth sciences, *Vestnik Rossijskoj akademii nauk*, 93(6), 518–525, <https://doi.org/10.31857/S0869587323060087> (in Russian).
- Gvishiani, A. D., I. N. Rozenberg, A. A. Soloviev, et al. (2023b), Electronic Atlas of Climatic Changes in the Western Russian Arctic in 1950-2021 as Geoinformatic Support of Railway Development, *Applied Sciences*, 13(9), 5278, <https://doi.org/10.3390/app13095278>.
- Gvishiani, A. D., I. N. Rozenberg, A. A. Soloviev, et al. (2023c), Study of the Impact of Climatic Changes in 1980-2021 on Railway Infrastructure in the Central and Western Russian Arctic Based on Advanced Electronic Atlas of Hydrometeorological Parameters (Version 2, 2023), *Russian Journal of Earth Sciences*, pp. 1–21, <https://doi.org/10.2205/2023es000882>.
- Han, Y., H. Revercomb, M. Crompt, et al. (2013), Suomi NPP CrIS measurements, sensor data record algorithm, calibration and validation activities, and record data quality, *Journal of Geophysical Research: Atmospheres*, 118(22), <https://doi.org/10.1002/2013JD020344>.
- Hocke, K., and N. Kämpfer (2009), Hovmöller diagrams of climate anomalies in NCEP/NCAR reanalysis from 1948 to 2009, *Climate Dynamics*, 36(1–2), 355–364, <https://doi.org/10.1007/s00382-009-0706-5>.
- Hovmöller, E. (1949), The Trough-and-Ridge diagram, *Tellus*, 1(2), 62–66, <https://doi.org/10.3402/tellusa.v1i2.8498>.

- Jury, M. R., B. Pathack, G. Campbell, B. Wang, and W. Landman (1991), Transient convective waves in the tropical SW Indian Ocean, *Meteorology and Atmospheric Physics*, 47(1), 27–36, <https://doi.org/10.1007/BF01025824>.
- Kasraei, A., A. H. S. Garmabaki, J. Odelius, et al. (2024), Climate change impacts assessment on railway infrastructure in urban environments, *Sustainable Cities and Society*, 101, 105,084, <https://doi.org/10.1016/j.scs.2023.105084>.
- Kattsov, V. M. (Ed.) (2022), *The Third Assessment Report on Climate Changes and Their Consequences on the Territory of the Russian Federation*, Naukoyemkie Tekhnologii, St. Petersburg (in Russian).
- Kim, E., C.-H. J. Lyu, K. Anderson, R. Vincent Leslie, and W. J. Blackwell (2014), S-NPP ATMS instrument prelaunch and on-orbit performance evaluation, *Journal of Geophysical Research: Atmospheres*, 119(9), 5653–5670, <https://doi.org/10.1002/2013JD020483>.
- Kostianaia, E. A., and A. G. Kostianoy (2023), Railway Transport Adaptation Strategies to Climate Change at High Latitudes: A Review of Experience from Canada, Sweden and China, *Transport and Telecommunication Journal*, 24(2), 180–194, <https://doi.org/10.2478/ttj-2023-0016>.
- Kostianaia, E. A., A. G. Kostianoy, M. A. Scheglov, A. I. Karelov, and A. S. Vasileisky (2021), Impact of regional climate change on the infrastructure and operability, *Transport and Telecommunication Journal*, 22(2), 183–195.
- Kovalenko, M. S., and E. V. Sibileva (2023), The Arctic's resource composition, production challenges and prospects, *The Arctic XXI century. Humanities*, (1(31)), 26–36, <https://doi.org/10.25587/SVFU.2023.44.59.003> (in Russian).
- Ma, H., J. Zeng, X. Zhang, et al. (2021), Evaluation of six satellite- and model-based surface soil temperature datasets using global ground-based observations, *Remote Sensing of Environment*, 264, 112,605, <https://doi.org/10.1016/j.rse.2021.112605>.
- Ministry of Transport of the Russian Federation (2023), Transport of Russia. Information and statistical bulletin. 2022 (in Russian).
- Overland, J. E., M. Wang, J. E. Walsh, and J. C. Stroeve (2014), Future Arctic climate changes: Adaptation and mitigation time scales, *Earth's Future*, 2(2), 68–74, <https://doi.org/10.1002/2013EF000162>.
- Post, E., R. B. Alley, T. R. Christensen, et al. (2019), The polar regions in a 2°C warmer world, *Science Advances*, 5(12), <https://doi.org/10.1126/sciadv.aaw9883>.
- Prants, S. V. (2021), Trench Eddies in the Northwest Pacific: An Overview, *Izvestiya, Atmospheric and Oceanic Physics*, 57(4), 341–353, <https://doi.org/10.1134/S0001433821040216>.
- Rankova, E. Y., O. F. Samokhina, and U. I. Antipina (2022), Features of the surface temperature regime over the Globe in 2021, *Fundamental and Applied Climatology*, 8(2), <https://doi.org/10.21513/2410-8758-2022-2-258-290> (in Russian).
- Rozenberg, I. N., I. A. Dubchak, M. N. Timoshenkova, and E. I. Zuravleva (2019), *Atlas of Railways*, Scientific Research and Design Institute of Informatization, Automation and Communication in Railway Transport, Moscow (in Russian).
- Russian Railways (2024a), Northern Railway, <https://szd.rzd.ru/ru/4858/page/103290?id=9491> (in Russian).
- Russian Railways (2024b), Oktyabrskaya Railway, <https://ozd.rzd.ru/ru/4009> (in Russian).
- Russian Railways (2024c), Sverdlovsk Railway, <https://svzd.rzd.ru/ru/4749/page/103290?id=5626> (in Russian).
- Rybikina, A., S. Hodson, A. Gvishiani, et al. (2018), CODATA and global challenges in data-driven science, *Russian Journal of Earth Sciences*, 18(4), 1–11, <https://doi.org/10.2205/2018ES000625>.
- Shokurov, M. V., and N. Y. Germankova (2015), Numerical simulation of gravity current propagation in a compressible atmosphere, *Physical Oceanography*, (4), <https://doi.org/10.22449/1573-160X-2015-4-53-65>.
- Surfer Help (2024), Minimum Curvature, https://surferhelp.goldensoftware.com/griddata/IDD_GRID_DATA_MINIMUM_CURVATURE.htm.
- Yagova, N. V., I. N. Rozenberg, A. D. Gvishiani, et al. (2023), Study of geomagnetic activity impact on functioning of railway automatics in Russian Arctic, *Arctic: Ecology and Economy*, 13(3), 341–352, <https://doi.org/10.25283/2223-4594-2023-3-341-352>.

Zonn, I. S., A. G. Kostianoy, and A. V. Semenov (Eds.) (2016), *The Eastern Arctic Seas Encyclopedia*, Springer International Publishing, Switzerland, <https://doi.org/10.1007/978-3-319-24237-8>.

Zonn, I. S., A. G. Kostianoy, and A. V. Semenov (Eds.) (2017), *The Western Arctic Seas Encyclopedia*, Springer International Publishing, Switzerland, <https://doi.org/10.1007/978-3-319-25582-8>.